

SANDIA REPORT

SAND2015-0729

Unlimited Release

Printed February 2015

Nitrogen Monitoring of West Hackberry 117 Cavern Wells

David L. Lord and Giorgia Bettin

Prepared by
Sandia National Laboratories
Albuquerque, New Mexico 87185 and Livermore, California 94550

Sandia National Laboratories is a multi-program laboratory managed and operated by Sandia Corporation, a wholly owned subsidiary of Lockheed Martin Corporation, for the U.S. Department of Energy's National Nuclear Security Administration under contract DE-AC04-94AL85000.

Approved for public release; further dissemination unlimited.



Sandia National Laboratories

Issued by Sandia National Laboratories, operated for the United States Department of Energy by Sandia Corporation.

NOTICE: This report was prepared as an account of work sponsored by an agency of the United States Government. Neither the United States Government, nor any agency thereof, nor any of their employees, nor any of their contractors, subcontractors, or their employees, make any warranty, express or implied, or assume any legal liability or responsibility for the accuracy, completeness, or usefulness of any information, apparatus, product, or process disclosed, or represent that its use would not infringe privately owned rights. Reference herein to any specific commercial product, process, or service by trade name, trademark, manufacturer, or otherwise, does not necessarily constitute or imply its endorsement, recommendation, or favoring by the United States Government, any agency thereof, or any of their contractors or subcontractors. The views and opinions expressed herein do not necessarily state or reflect those of the United States Government, any agency thereof, or any of their contractors.

Printed in the United States of America. This report has been reproduced directly from the best available copy.

Available to DOE and DOE contractors from

U.S. Department of Energy
Office of Scientific and Technical Information
P.O. Box 62
Oak Ridge, TN 37831

Telephone: (865) 576-8401
Facsimile: (865) 576-5728
E-Mail: reports@adonis.osti.gov
Online ordering: <http://www.osti.gov/bridge>

Available to the public from

U.S. Department of Commerce
National Technical Information Service
5285 Port Royal Rd.
Springfield, VA 22161

Telephone: (800) 553-6847
Facsimile: (703) 605-6900
E-Mail: orders@ntis.fedworld.gov
Online order: <http://www.ntis.gov/help/ordermethods.asp?loc=7-4-0#online>



Nitrogen Monitoring of West Hackberry 117 Cavern Wells

David L. Lord and Giorgia Bettin
Geotechnology & Engineering Department
Sandia National Laboratories
P.O. Box 5800
Albuquerque, New Mexico 87185-MS0706

Abstract

U.S. Strategic Petroleum Reserve (SPR) oil storage cavern West Hackberry 117 was tested under extended nitrogen monitoring following a successful mechanical integrity test in order to validate a newly developed hydrostatic column model to be used to differentiate between normal “tight” well behavior and small-leak behavior under nitrogen. High resolution wireline pressure and temperature data were collected during the test period and used in conjunction with the hydrostatic column model to predict the nitrogen/oil interface and the pressure along the entire fluid column from the bradenhead flange nominally at ground surface to bottom of brine pool. Results here and for other SPR caverns have shown that wells under long term nitrogen monitoring do not necessarily pressurize with a relative rate (P_{N_2}/P_{brine}) of 1. The theoretical relative pressure rate depends on the well configuration, pressure and the location of the nitrogen-oil interface and varies from well to well. For the case of WH117 the predicted rates were 0.73 for well A and 0.92 for well B. The measured relative pressurization rate for well B was consistent with the model prediction, while well A rate was found to be between 0.58-0.68. A number of possible reasons for the discrepancy between the model and measured rates of well A are possible. These include modeling inaccuracy, measurement inaccuracy or the possibility of the presence of a very small leak (below the latest calculated minimum detectable leak rate).

ACKNOWLEDGMENTS

The authors wish to thank Mark McCoy (Fluor Federal Petroleum Operations) field support during this study, and Lisa Eldredge (Fluor Federal Petroleum Operations) and David Rudeen (GRAM, Inc.) for technical reviews.

CONTENTS

Acknowledgments	4
Nomenclature.....	10
1 Executive Summary	11
2 Problem Statement	13
2.1 Scope of Report.....	13
3 Background	14
3.1 SPR Cavern Pressure Monitoring	14
3.2 Cavern Pressurization Behavior under Nitrogen	15
3.3 Big Hill Cavern Behavior under Nitrogen	17
3.3.1 Related Study from Literature	18
3.4 Dome Geology	20
3.5 Cavern History	21
4 Methodology	23
4.1 Hydrostatic Column Model.....	23
4.1.1 Model Domain	23
4.1.2 Fluid Pressure Model	24
4.1.3 Predicting Nitrogen-Oil Interface Depths.....	24
4.1.4 Predicting Pressure Change at the Gas Wellhead with Creep Closure.....	25
4.2 Data Acquisition and Processing	26
4.2.1 Hourly Wellhead Pressure	26
4.2.2 Temperature Effect on Instrumentation.....	27
4.2.3 Wireline Data.....	27
4.3 Nitrogen Test Configuration	31
5 Analysis of Cavern Monitoring.....	32
5.1 Wellhead Pressure Data	32
5.1.1 Cemented Annulus Pressures	35
5.1.2 Neighbor Cavern Activity.....	38
5.2 2014 MIT on WH117.....	39
5.3 Long Term Nitrogen Monitoring Test Logs	39
5.3.1 Interface Depth Interpretation from Logs.....	40
5.3.2 Well A Logs.....	41
5.3.3 Well B Logs.....	44
6 Hydrostatic Column Model Results	46
6.1 Model Parameters	46
6.2 Model Predictions	47
6.3 Possible Source of Discrepancy	50

6.4	Model Estimates for Possible N ₂ Leak Rates.....	51
6.4.1	Well A simulations	51
6.4.2	Well B	54
7	Conclusion.....	56
8	Cited References.....	57
9	Appendix: Well Drawings.....	58
10	Appendix: Logs	65
11	Appendix: Oil Quality	67
12	Appendix: Model Well Geometry	68
13	Appendix: Conversions	70
	Distribution	70

FIGURES

Figure 3-1: Schematic of typical pressure monitoring configuration for SPR two-well cavern in (a) normal operations, and (b) under nitrogen monitoring.	14
Figure 3-2: Wellhead pressures for SPR cavern Big Hill 112 for period Sept 1, 2013 through March 16, 2014. Cavern was under extended nitrogen monitoring during this period.	16
Figure 3-3: Schematic of top of 47 MB brine cavern, reproduced from Berest, Brouard et al. (2002).	19
Figure 3-4: Excerpt from table 3 in Berest, Brouard et al. (2002) showing computed and measured nitrogen wellhead, P_g equivalent to $P(N_2)$ and brine wellhead, P_b equivalent to $P(\text{brine})$ pressure changes upon injection and withdrawal of brine.	19
Figure 3-5: West Hackberry salt dome. Small circles represent the footprint of the cavern Grid size is 5000ft. Contours show top of salt depth, below land surface.	20
Figure 3-6: Image from the 2013 Sonar of WH117.	21
Figure 3-7: Coefficient of variation of the casing diameter obtained from the MultiArm Caliper (MAC) survey of July 2010. Image shows a zone of increased ovality around 2200 ft and 2275 ft.	22
Figure 4-1: Logical diagram of computational mesh used in hydrostatic column model.	23
Figure 4-2: Graphical model output showing intersection of pressure curves indicating predicted N_2 -Oil interface depth.	25
Figure 4-3: Temperature measured at the well pad for WH117 during the nitrogen testing. Included in the figure are the atmospheric temperature observed at Lake Charles regional Airport, LA. http://www.friendlyforecast.com	27
Figure 4-4: Wireline tool used to collect fluid properties during logging operation with temperature probe indicated.	28
Figure 4-5: Schematic of the combined wireline tool run at special test initialization (Mar 27, 2014) and finalization (Apr 23, 2014) on WH117A and B.	30
Figure 4-6: Conceptual sketch of the cavern during the extended nitrogen test. Note A-side NOI is inside the casing (ID ~ 1 ft), while the B-side NOI is in the salt chimney (ID ~ 4 ft).	31
Figure 5-1: Wellhead pressure history for cavern WH117 from Nov. 2013 to May 2014.	32
Figure 5-2: Wellhead pressure for WH117A under long-term nitrogen monitoring.	33
Figure 5-3: Wellhead pressure for WH117B under long-term nitrogen monitoring.	33
Figure 5-4: Illustration of pressurization rates for WH117A (right) and 117B (left). The vertical lines bound the data that has been fit for comparison.	34
Figure 5-5: Well head pressure of WH117A superimposed on temperature data also measured at the well head.	35
Figure 5-6: Wellbore pressure as it compares to the cemented annulus pressure for BM004B.	36
Figure 5-7: Pressure of the cemented annulus in well WH117A for the past six months as they compared to the pressure inside the casing.	37
Figure 5-8 Pressure of the cemented annulus in well WH117B for the past six months compared to the pressure inside the casing.	37
Figure 5-9: plan view of West hackberry cavern field. WH117 is circled in red, and nearest neighbor caverns are circled in blue.	38
Figure 5-10: Pressure history of WH117 neighboring caverns during the nitrogen test.	39
Figure 5-11: High resolution pressure log for WH117A around the expected NOI depth. Log conducted on Mar 27, 2014.	40

Figure 5-12: Logs results for WH117A. Initialization log ran on March 27, 2014, finalization on April 23, 2014.	41
Figure 5-13: WH117A close up view of pressure log results highlighting the NOI movement during the test	42
Figure 5-14: Close up view of WH117A Temperature logs for long term nitrogen monitoring test.....	43
Figure 5-15: Logs results for WH117B. Initialization log ran on Mar 27, 2014, finalization on Apr 23, 2014.	44
Figure 5-16: Close up view of WH117B Temperature logs for long term nitrogen monitoring test.....	45
Figure 6-1: Fluid density calculated in the hydrostatic model as it compared to logging data from March 2014.....	47
Figure 6-2: Graphics of the difference between measured pressure data from the log (as a function of depth) at initialization of the test, vs. the predicted pressure from the model.	48
Figure 6-3: Wellhead pressure (left) and NOI (right) for WH117A and B as predicted from the nitrogen column model and compared to the measured values.....	49
Figure 6-4: Wellhead pressure prediction for WH117A as a function of the change in cavern pressure. Listed on the table on the right are the relative pressurization rates and the corresponded apparent leak rates.....	52
Figure 6-5: Pressure prediction as a function of time for WH117A. Inset view shows model predictions during the nitrogen test as it compared to the observed wellhead pressure data.	53
Figure 6-6: Prediction of the NOI movement for a range of simulated leak rates. Table illustrates how an uncertainty of ± 0.5 ft in the NOI measurement can lead to an estimated leak rates that varies between 17.3-22.5 bbl/yr.....	54
Figure 6-7: Wellhead pressure prediction for WH117B. (right) table with the simulated leak rate and resultant relative pressurization rate.	54
Figure 6-8: WH117B NOI predictions for a tight well (blue) and a simulated leak (red) of 26.1 bbl/yr. Dashed line corresponds to the Casing Shoe Depth.....	55
Figure 9-1 West Hackberry 117A, Well Completion Configuration Drawing, WH-M-123-041, 5/5/2014	58
Figure 9-2 Well completion drawing of WH117B, updated on 5/5/2014.	59
Figure 9-3. Big Hill-112A, Well Completion Configuration, Drawing BH-M-123-023, version 5, 1/10/2011.....	60
Figure 9-4. Big Hill 112B, Well Completion Configuration Drawing, BH-M-123-024, 1/10/2011.....	61
Figure 9-5. West Hackberry 117A, Wellhead Configuration Drawing, WH-M-122-041, 2/21/2007	62
Figure 9-6. West Hackberry 117A, Wellhead Configuration Drawing, WH-M-122-042, 2/22/2007	63
Figure 9-7. WH117, Piping and Instrument Drawing, WH-M-103-127, 12/5/2011	64
Figure 10-1. Temperature logs for WH117A since December 2013.....	65
Figure 10-2. Temperature logs for WH117B since December 2013.....	66

TABLES

Table 1-1. Relative pressurization rates for WH117A and B predicted by the hydrostatic model as they compare to the experimental data.....	11
--	----

Table 3-1: Slopes of BH112 pressurization curves from Figure 3-2 evaluated between Dec 28, 2013 and Feb 25, 2014.....	16
Table 3-2. Listing of Big Hill caverns under extended nitrogen monitoring during the period Nov 2012 – Jun 2014.	17
Table 3-3. Representative pressurization rates for Big Hill caverns under extended nitrogen monitoring.....	18
Table 3-4. Representative pressurization rates for Big Hill caverns under mechanical integrity testing (MIT).....	18
Table 3-5: Timeline of selected WH117 events, and logs.....	22
Table 4-1: Labels for pressure and temperature channel per well head drawings.....	26
Table 5-1: Pressurization rates relative to brine calculated between April 16-22, 2014.	34
Table 5-2: Summary of results from MIT logs.....	39
Table 5-3: Pressures and NOI of the long-term nitrogen monitoring test at initialization and finalization as reported by the logs.....	40
Table 6-1: List of parameters used in the hydrostatic column model.....	46
Table 6-2: Model predictions for the wellhead pressure and NOI for both wells. The value of pressure at initialization was set to match.	49
Table 6-3: Relative pressurization rates for WH117A and WH117B predicted by the hydrostatic column model as they compare to the experimental data.....	49
Table 6-4: Summary of predicted pressurization rates as a function of calculated leak rates. N ₂ leak rate volumes [bbl/yr] in column 1 are given at casing seat depth P, T conditions.	51
Table 11-1. Crude oil inspection analysis for WH117 (July, 2002).....	67
Table 12-1. West Hackberry 117A well geometry.....	68
Table 12-2. West Hackberry 117B well geometry.....	69

NOMENCLATURE

BH	Big Hill SPR Site
BHF	Braden Head Flange
CCL	Casing Collar Locator
CSD	Casing shoe depth
DCS	Distributed Control System
DOE	Department of Energy
FFPO	Fluor Federal Petroleum Operations
ID	Internal diameter
MAC	Multi-Arm Caliper
MIT	Mechanical integrity test
MMB	Million barrels
NOI	Nitrogen Oil interface
OBI	Oil Brine Interface
OD	Outer diameter
SNL	Sandia National Laboratories
SPR	Strategic Petroleum Reserve
TD	Total depth
WH	West Hackberry SPR Site

1 Executive Summary

This report documents a special test of U.S. Strategic Petroleum Reserve (SPR) cavern storage wells West Hackberry 117A and B under nitrogen after a routine mechanical integrity test (MIT) in order to better understand normal cavern pressure behavior under extended nitrogen monitoring. Both wells passed the MIT in January 2014, indicating that gas leak rates were at or below detection limits before the special test began in March, 2014. The test duration was one month, and data were collected hourly at the wellhead and then via wireline at the beginning of the test on March 27, 2014, and at the end of the test on April 23, 2014.

The test was designed to help delineate between normal “tight” well behavior and small-leak behavior under extended nitrogen testing. Current observations of wellhead pressurization data for suspected small-leak Big Hill caverns under special nitrogen monitoring starting in November, 2012, indicate steady, yet distinct, pressurization rates for different wells within the same cavern. The wells under nitrogen (slick well and static annulus) pressurize at about 2/3 the rate of a well under liquid (hanging string). The initial position of the SPR well integrity working group was that the slower re-pressurization of the wells under gas relative to those under liquid indicated slow fluid leaks from the cased wells. Subsequent modeling has indicated that the differences may be due to basic fluid physics in a non-leaking system. Behavior here is driven by the several order-of-magnitude disparities in fluid compressibility between gas and liquid in a cavern-scale manometer configuration subjected to constant creep closure during the test period. The extended nitrogen testing in the WH117 wells that had just passed MIT were considered a good starting point for an experimental non-leak control group.

The special test set the nitrogen-oil interface (NOI) level at nominally 1650 ft depth in the WH117A-well (slick hole) and at the MIT depth right below the casing shoe at about 2419 ft depth in the WH117B-well. Hourly pressure monitoring revealed that Well B under nitrogen pressurized at a rate very similar to that of brine in the hanging string, at a relative rate between 0.9 and 1.0. Well A under nitrogen behaved differently, pressurizing at a relative rate between 0.6-0.7 that of brine. A hydrostatic model configured to simulate the WH117 test conditions predicted similar behavior, returning a theoretical relative pressurization rate of 0.92 for the B-well under nitrogen, and 0.73 for the A-well under nitrogen. Data-model comparisons are summarized in Table E-1. The disparity between theoretical and measured rates in well A may be due to modeling inaccuracy, data acquisition inaccuracy or be indicative of a small gas leak below the minimum detectable leak rate (MDLR) in the MIT, but detectable during special nitrogen testing. The leak would also have to be located above the Nitrogen Oil Interface (NOI) depth, and not at the casing shoe. More details are given in the report.

Table 1-1. Relative pressurization rates for WH117A and B predicted by the hydrostatic model as they compare to the experimental data.

	WH117A N2	WH117B N2	WH117B Brine
P(oil)/P(B, brine) (model)	0.732	0.924	1
P(oil)/P(B, brine) (experiment)	0.58-0.68	0.90-1.0	1

The important distinguishing factors between the B-well and A-well driving the pressurization rate behavior were:

- the NOI setting depths were ~1650 ft for well A and ~2419 ft for well B, and
- the corresponding well diameters at the NOI were ~1 ft for well A and ~4 ft for well B

For the same increase in cavern brine pressure, the NOI displaced measurably (several feet) in well A, and less than a foot (below wireline detection limits) in well B. The resulting impacts on wellhead pressurization as propagated through the manometer effects are that well A only pressurizes at something like 2/3 that of brine, where well B pressurizes at nearly equal rate to brine. This is the same effect seen at Big Hill where selected caverns have been under nitrogen monitoring for a period of months to years. The NOI was set near the salt-caprock interface around 1600-1700 ft. The cased hole is about 1 ft diameter in this region, and the interface moves measurably with normal cavern creep over weeks to months. This is also consistent with the observation that many Big Hill SPR caverns show a relative pressurization rate near 1.0 during MIT, but then show a measurably lower relative rate near 0.7 during extended nitrogen monitoring. Recall during MIT, the NOI is necessarily placed below the casing shoe in the salt chimney, where the diameter is highly variable and interface movement is considerably less than up in the cased hole for the same increase in brine pressure. If the nitrogen pressure in an MIT tracks at a fraction of the brine rate and the interface that starts below the casing shoe in a wide salt chimney moves up measurably, this is a real cause for concern and the MIT would not pass.

The implication for SPR is that data and modeling so far indicate that some disparity in pressurization rate for wells under nitrogen relative to wells under brine is to be expected, in particular if the NOI is set up in the cased hole and monitored for a period of weeks to months. A theoretical relative pressurization rate of ~0.7 was calculated from a numerical model for the WH117A configuration, which should also hold true for the selected Big Hill wells (BH112, BH107, BH103) currently or recently under extended monitoring. While the focus of this report was on WH117, Sandia intends to expand the study in a subsequent SAND report to all the Big Hill wells under nitrogen in the last several years to build a more robust and widely applicable theory and model that may assist in delineating normal tight-well behavior from small leak behavior under nitrogen.

2 Problem Statement

U.S. Strategic Petroleum Reserve (SPR) West Hackberry storage cavern 117 (WH117) was held under extended nitrogen monitoring in the months following a successful Mechanical Integrity Test (MIT) in order to monitor the nitrogen wellhead pressures and interface levels during a steady creep closure period. This test was run in order to help delineate between normal “tight” well behavior and small-leak behavior under extended nitrogen testing.

Current observations of wellhead pressurization data for suspected small-leak SPR caverns at the Big Hill storage facility under special nitrogen monitoring indicate steady, yet distinct, pressurization rates for different wells within the same cavern. The wells under nitrogen (slick well and static annulus) with the interface placed up at the salt-caprock interface pressurize at about 70% the rate of a well under liquid (hanging string). The initial position of the SPR well integrity working group was that the slower re-pressurization of the wells under gas relative to those under liquid indicated slow fluid leaks from the cased wells. Subsequent modeling has indicated that the differences may be due to basic fluid physics in a non-leaking system, with behavior driven by the several order-of-magnitude disparities in fluid compressibility between gas and liquid in a cavern system subjected to constant creep closure during the test period. The well geometry and location of the gas-liquid interface relative to changes in borehole diameter are also important factors.

2.1 Scope of Report

This report examines the behavior of SPR cavern WH117 from Nov 2013 – Apr 2014 during which time the cavern wells were held under nitrogen. Wellhead pressures and wireline data to include nitrogen-oil interface, oil-brine interface, high-resolution fluid pressure, and fluid temperatures were measured and compared against model simulations.

3 Background

3.1 SPR Cavern Pressure Monitoring

A typical SPR oil storage cavern containing two wells has continuous product and brine wellhead monitoring under normal operating conditions as indicated Figure 3-1(a). Oil is typically moved in and out of the cavern through the “slick hole” well that does not contain a hanging string, and this oil pressure is indicated by $P(A,Oil)$ in Figure 3-1(a). Brine and/or water is moved in and out of the cavern through the hanging string, with pressure indicated by $P(B,brine)$ in Figure 3-1(a). Oil is also contained and monitored in the annular space between the hanging string and cemented casing in well B, sometimes called the “static annulus” with pressure $P(B,oil)$.

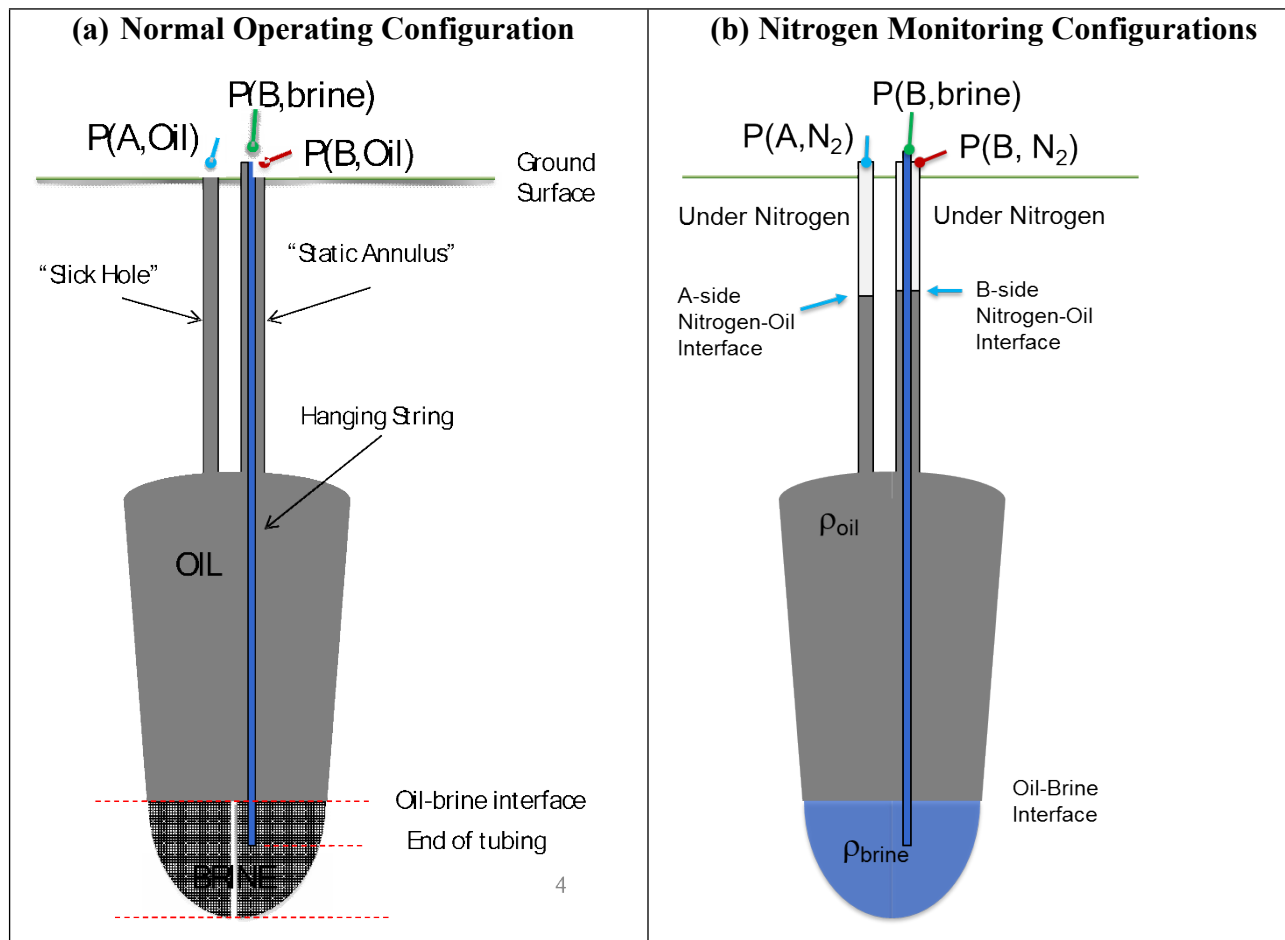


Figure 3-1: Schematic of typical pressure monitoring configuration for SPR two-well cavern in (a) normal operations, and (b) under nitrogen monitoring.

The same two-well SPR cavern under nitrogen monitoring is depicted conceptually in Figure 3-1(b), where nitrogen has been pumped into one or both the slick hole and the static annulus, with pressure indicated by $P(A,N_2)$ and $P(B,N_2)$ respectively. Brine pressure in the hanging string is indicated by $P(B,brine)$. Generally speaking, the volume of nitrogen used to pressurize the wells is small enough that the brine pressure $P(B,brine)$ and oil-brine interface depth (OBI) are

insensitive to this change. Conversely, the product wellhead pressures rise markedly as nitrogen is injected to displace oil down the wellbore. Well completion configuration drawings for the subject cavern of this report, WH117, are given in Appendix Well Drawings (WH-M-123-041, WH-M-123-042).

Since all SPR wells have multiple nested casings starting from the ground surface, there is at least one more pressure monitoring point in the first cemented annulus (see Appendix Well Completion Drawings: Wellhead Configuration WH117A, Wellhead Configuration WH117B). The cemented annulus pressure is not currently addressed in any of the cavern modeling discussed herein, but it is used as an indicator of the integrity of the innermost casing, and is discussed later in this report. Cemented casing pressures are expected to show very low or zero (gauge) values, independent of the product side pressures. If the annulus pressure responds to product pressure, then primary containment of the product (oil) or test fluid (nitrogen) has been lost.

3.2 Cavern Pressurization Behavior under Nitrogen

SPR caverns gradually pressurize due to salt creep closure and geothermal heating. This behavior is monitored and modeled to support daily SPR operations level using an approach documented in a series of reports describing the CAVEMAN application (Ballard and Ehgartner (2000); Ehgartner (2003); Ehgartner (2004)). Adding nitrogen to the top of the oil wells changes the physics, and there has been no documented effort prior to this report to observe and model SPR caverns under nitrogen for periods of months.

Operational experience at SPR holding caverns under extended nitrogen monitoring shows that following a startup transient of a few weeks, caverns with small or zero leak rates that are at or below detection thresholds settle into reproducible trends for wellhead pressurization, with typical behavior shown in Figure 3-2. The cavern selected here for illustration, BH112, has had both cavern wells under nitrogen since November 2012, following abnormal pressure behavior that caused concern for a possible cemented casing leak. The nitrogen-oil interface depths were set to about 1700 ft, which is inside the cemented 10.75 in (OD) steel casing and about 60 to 70 ft below the salt-caprock interface (see Appendix Well Completion Drawings: BH112A Well Completion Configuration, BH-112B Well Completion Configuration). The interfaces were positioned at this depth because the salt-cap interface corresponds to the region of maximum observed deformation in cased wells at Big Hill, and several conspicuous well failures have occurred in this region.

The figure shows wellhead pressure monitoring for both A and B nitrogen wells (scale on left axis) and the brine well (scale on right axis) for a period Sept 1, 2013 through March 16, 2014. One full pressurization cycle is captured, starting around Sept 27, 2013 and ending around Mar 1, 2104. The brine wellhead pressure **P(B,brine)** rises at a faster rate than either of the nitrogen wellheads. The rates were evaluated using a simple linear fit slope function and compared in Table 3-1 below. The brine well pressure increased at approximately 0.48 psi/day, while the nitrogen well pressures both increased at 0.34 psi/day. The relative ratios of nitrogen wellhead to brine wellhead pressurization were approximately 0.7. This ratio was consistent through several cavern cycles, as well as for other Big Hill caverns (BH103, BH107) in similar configurations under extended nitrogen monitoring.

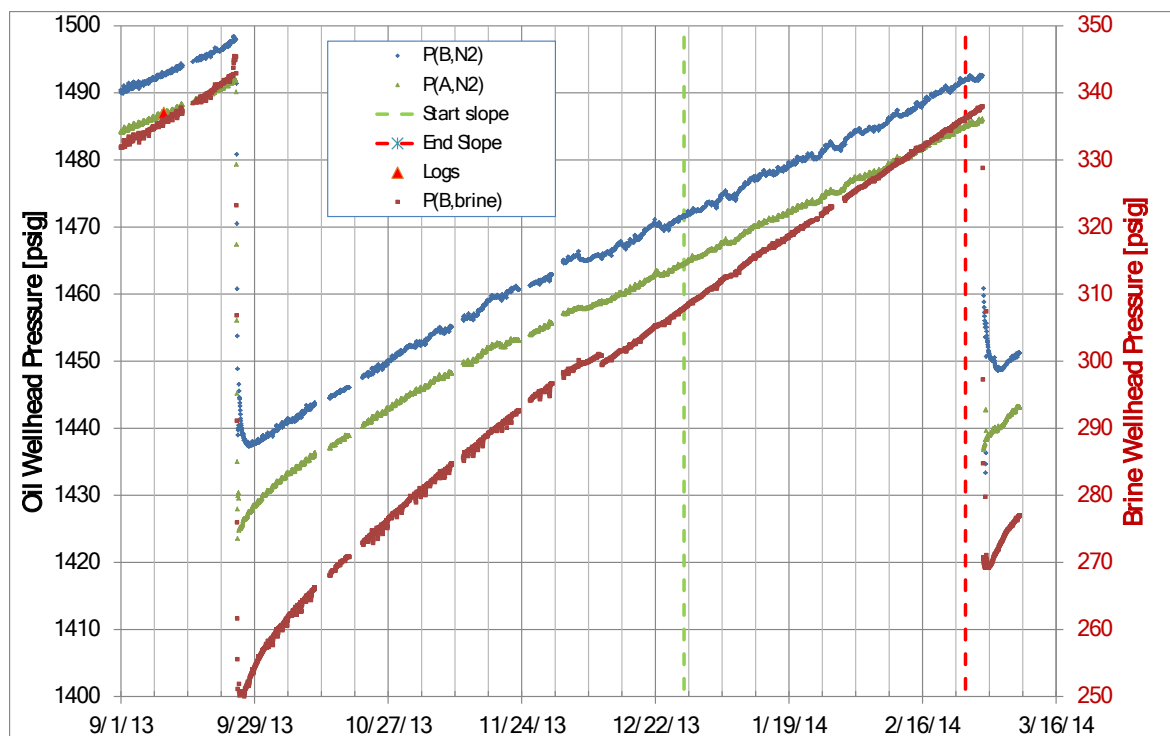


Figure 3-2: Wellhead pressures for SPR cavern Big Hill 112 for period Sept 1, 2013 through March 16, 2014. Cavern was under extended nitrogen monitoring during this period.

Table 3-1: Slopes of BH112 pressurization curves from Error! Reference source not found. evaluated between Dec 28, 2013 and Feb 25, 2014.

	P(B,N2)	P(B,brine)	P(A,N2)
Slope [psi/day]	0.34	0.48	0.34
R² - square of correlation coefficient	0.99	1.00	1.00
Ratio to Brine	0.71	1.00	0.72

Competing theories were posed within the SPR technical community for explaining why the relative pressurization ratio was 0.7 instead of 1.0, which is more routinely observed in cavern integrity tests under nitrogen. One theory was that the wells under nitrogen in the extended monitoring were leaking enough nitrogen mass to lag behind the brine pressurization rate. Another theory was that fluid physics, namely the differences between gas and liquid compressibilities in a manometer configuration could explain these differences. Yet another theory suggested that the position of oil-nitrogen interface above or below the casing shoe could play a defining role in how closely the gas pressurization would parallel the brine pressurization. Most of the wells at Big Hill (BH103, 107, 112) cited as showing the 0.7 relative pressurization rate were put under nitrogen because they had exhibited some abnormal pressurization behavior.

As such, they were suspected of leaking from the very beginning, and may not serve as good models for normal tight well behavior.

The current test in WH117 was designed to help delineate what a “tight” well pressurization response will be when the nitrogen oil-interface is set to the salt-cap interface region over time period of weeks to months, and necessarily after the start-up transient. In this way, the test serves as an experimental control to establish what expected tight behavior should look like.

3.3 Big Hill Cavern Behavior under Nitrogen

The U.S. Strategic Petroleum Reserve (SPR) has been holding nitrogen on several cavern storage wells since Nov 2012. A listing of caverns at the Big Hill site under nitrogen monitoring is given in Table 3-2. The wells in question exhibited some level of anomalous pressurization behavior in the last year that caused concern for their near-term pressure integrity.

Table 3-2. Listing of Big Hill caverns under extended nitrogen monitoring during the period Nov 2012 – Jun 2014.

Cavern Wells	Start	Comment	End	Comment
BH112-A,B	Nov, 2012	N ₂ injected due to abnormal cavern pressurization behavior in Oct, 2012	Ongoing	Still under N ₂ monitoring
BH103-A,B	Nov, 2012	N ₂ injected due to abnormal cavern pressurization behavior in Oct, 2012	Dec, 2013	Installed cemented liner in B-well. N ₂ re-injected for post-remediation MIT and still under monitoring as of June 2014.
BH107-A,B	Dec, 2013	N ₂ injected due to abnormal cavern pressurization behavior in Dec, 2013	Ongoing	Still under N ₂ monitoring

Nitrogen provides several benefits in this scenario:

- as a buffer fluid that separates the product (crude oil) from the possible leak zone and loss to the environment, and
- as a sensitive diagnostic to identify the presence and location of a leak.

SPR cavern pressures rise steadily with time due to salt creep and geothermal heating. Wellhead pressures are measured continuously and pressurization rates are analyzed for information regarding the integrity of the storage system. This holds true for all storage wells, independent of whether they contain brine, oil, and/or have nitrogen caps.

Observed pressurization rates for the Big Hill caverns listed above in Table 3-2 under extended nitrogen monitoring are shown in Table 3-3. Noteworthy for this discussion is that the relative pressurization rates (nitrogen-capped well versus brine well) shown in the far right columns for all wells over all selected date ranges show consistent values of 0.66 – 0.70 ($\mu = 0.68$, $\sigma = 0.01$). This behavior is distinct from MIT’s, in that the relative pressurization rates observed during the MIT’s are closer to 1.0 (range 0.71 – 1.19 with $\mu = 0.98$, $\sigma = 0.17$). This is illustrated upon

comparing the extended monitoring data in Table 3-3 and against the relative rates shown for MIT's in Table 3-4.

Table 3-3. Representative pressurization rates for Big Hill caverns under extended nitrogen monitoring.

Cavern	Date Range		Pressurization Rate [psi/day]			Relative Rate to Brine	
	<i>Start Date</i>	<i>End Date</i>	<i>Well A-N₂</i>	<i>Well B-N₂</i>	<i>Well B-brine</i>	<i>Well A-N₂</i>	<i>Well B-N₂</i>
BH107	3/15/2014	5/10/2014	0.33	0.33	0.47	0.70	0.69
BH103	5/10/2013	7/15/2013	0.58	0.58	0.85	0.68	0.68
BH103	8/1/2013	10/15/2013	0.69	0.67	1.00	0.69	0.67
BH112	11/15/2012	3/1/2013	0.32	0.33	0.49	0.66	0.67
BH112	4/1/2013	9/1/2013	0.32	0.32	0.47	0.69	0.69

Table 3-4. Representative pressurization rates for Big Hill caverns under mechanical integrity testing (MIT).

Cavern	Date Range		Pressurization Rate [psi/day]			Relative Rate to Brine	
	<i>Initialization Date</i>	<i>Finalization Date</i>	<i>Well A-N₂</i>	<i>Well B-N₂</i>	<i>Well B-brine</i>	<i>Well A-N₂</i>	<i>Well B-N₂</i>
BH107	3/29/2010	4/5/2010	0.34	0.38	0.32	1.09	1.19
BH103	8/16/2012	8/30/2012	0.58	0.68	0.64	0.92	1.08
BH112	2/21/2010	3/6/2010	0.41	0.54	0.58	0.71	0.93

The disparities in pressurization behavior in nitrogen-capped wells during extended nitrogen monitoring versus MIT raised some questions that require further investigation. Is the 0.7 relative pressurization rate observed in the extended nitrogen monitoring an indicator of small leaks in the cemented casing? Why would these same leaks not be detected in the MIT? What is the expected pressurization behavior for a gas-tight well? The experiment detailed in this report is designed to address these questions. In addition, a hydrostatic column model with compressible fluids was developed to help understand the basic physics in this system.

3.3.1 Related Study from Literature

Berest, Brouard et al. (2002) conducted a field test on a 47 MB salt cavern filled with brine and capped with nitrogen that is instructive in this discussion. A schematic of the top of the cavern is shown in Figure 3-3. The study injected and removed 200L (1.26 bbl) of brine, and measured the pressure changes in the nitrogen-capped and brine wellheads. These pressure changes are indicated in Figure 3-4 (reproduced from Berest, Brouard et al. (2002)). This process of adding and removing small amounts of brine is similar to the effects of creep closure on the SPR caverns.

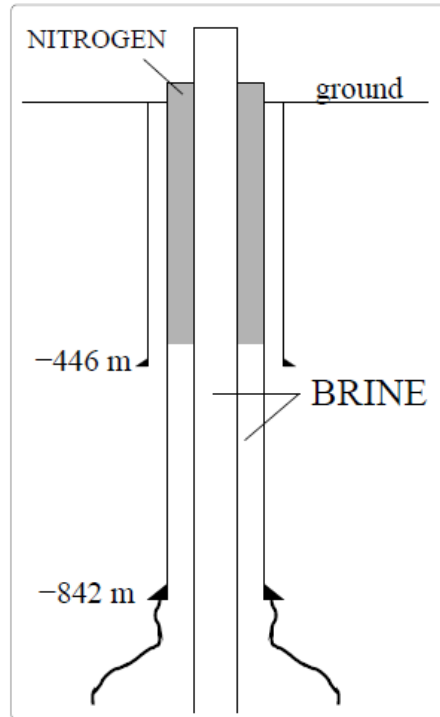


Figure 3-3. Schematic of top of 47 MB brine cavern, reproduced from Berest, Brouard et al. (2002).

	Brine Injection		Brine Withdrawal	
	Computed	Measured	Computed	Measured
ΔP_b (kPa)	+60	+67	-60	-67
ΔP_g (kPa)	+34	+38	-35	-35

Figure 3-4. Excerpt from table 3 in Berest, Brouard et al. (2002) showing computed and measured nitrogen wellhead, P_g equivalent to $P(N_2)$ and brine wellhead, P_b equivalent to $P(\text{brine})$ pressure changes upon injection and withdrawal of brine.

The effects on the measured brine $P(\text{brine})$ and nitrogen $P(N_2)$ wellheads were as follows:

- Brine injection caused measured $P(N_2)$ to increase 38 kPa, compared to 67 kPa for the brine. This is a relative rate of $38/67 = 0.57$.
- Brine withdrawal caused $P(N_2)$ to decrease 35 kPa, compared to 67 kPa for the brine. This is a relative rate of $35/67 = 0.52$.
- Associated modeling found comparable results, with relative ratios of $34/60 = 0.57$ for injection and $35/60 = 0.58$ for withdrawal.

Using the information gathered from Berest, Brouard et al. (2002) paper (well geometry, pressures, etc.) the Sandia hydrostatic column model discussed below in section 4.1 computed a relative pressurization rate of 0.63. While it's difficult to find the cause of the small variation between the published rates from Berest and the one we estimated, both rates are decidedly lower

than 1.0. The authors believe there is a theoretical basis for expecting the gas wellhead pressurization rates to be lower than brine when the liquid-gas interface is located in the relatively narrow cased well section.

3.4 Dome Geology

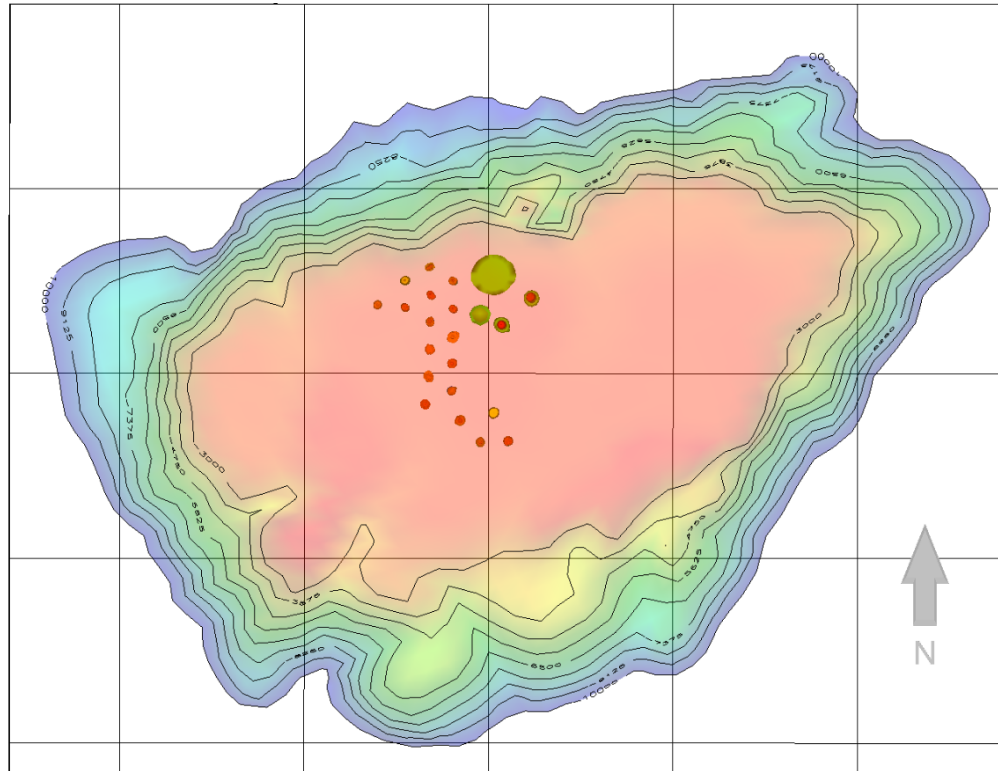


Figure 3-5: West Hackberry salt dome. Small circles represent the footprint of the cavern. Grid size is 5000ft. Contours show top of salt depth, below land surface.

Cavern WH117 is situated in the West Hackberry salt dome, one of the largest domes along the Gulf Coast and located in southwest Louisiana. The dome is elliptical in shape and is approximately 4 miles across NE-SW and 2 miles wide N-S (Figure 3-5). The dome is part of a salt ridge comprising of both West Hackberry and East Hackberry salt domes, with East Hackberry being located directly to the east. The top of salt is at a depth of approximately 2000 ft. The salt is relatively pure consisting of halite with 3 % anhydrite locally. The overlying caprock is approximately 500 ft thick with the top of caprock at a depth of 1500 ft. Specifically, at the location of WH117, drilling operations found the caprock at 1594ft from the Braden Head Flange (BHF)¹ ft, and top of salt at 2051 ft. Salt core and drill cuttings from WH117A and B wells showed a homogeneous salt with no unusually high concentration of anhydrite as consistent with the rest of the dome.

3.5 Cavern History

West Hackberry cavern 117 is a phase 2 cavern constructed by SPR in the early 80s. Specifically, the completion of well A ended in December 1983 to a total depth (TD) of 5054 ft.

¹ All depth reported in this report are measured from the BHF

During drilling no major zones of lost circulation were found even though a slight loss of mud was encountered at the top of caprock. The final casing of 13 3/8 in was cemented to a depth of 2415 ft (Franks 1984a). Well 117B was finished in March 1984, but it did encounter lost circulation problems at 1676 ft. After using 7 different lost circulation pills and 2 cement plugs the drilling was resumed, and TD of 5012 ft was reached. The final casing (13 3/8 in) reached a depth of 2410 ft (Franks 1984b). No gas was encountered while drilling of either well. Leaching began in Jun 1985 and was completed in Oct 1988. MIT's were conducted every 5 years since the cavern was completed; Mar 1989, Mar 1994, Jan 2004, Mar 1999, Jan 2004 and the latest in Jan 2014. All MIT's passed and no remediation was ever carried out leaving the well configurations as originally installed. Completion drawings for both wells are included in the appendix. The latest sonar was conducted in 2013 through well A (slick well) and the resultant schematic is shown Figure 3-6. A multi-arm caliper log was run in Jul 2010 on the A well. Casing diameter measurements were processed and a coefficient of variation, defined as the standard deviation normalized by the mean, was calculated as a function of depth. Despite finding some ovality at 2200 ft and 2275 ft (see Figure 3-7) the overall condition of the casing was reported to be 'very good'. The salt-caprock interface near 1637 feet does not appear to be associated with any notable deformation, which has shown to be a critical region in the several Big Hill caverns that developed casing leaks. The sum of these observations from the drilling history, MIT's, and 2010 MAC create no expectations that the WH117 wells should exhibit leakage greater than the sensitivity level of the MIT's.

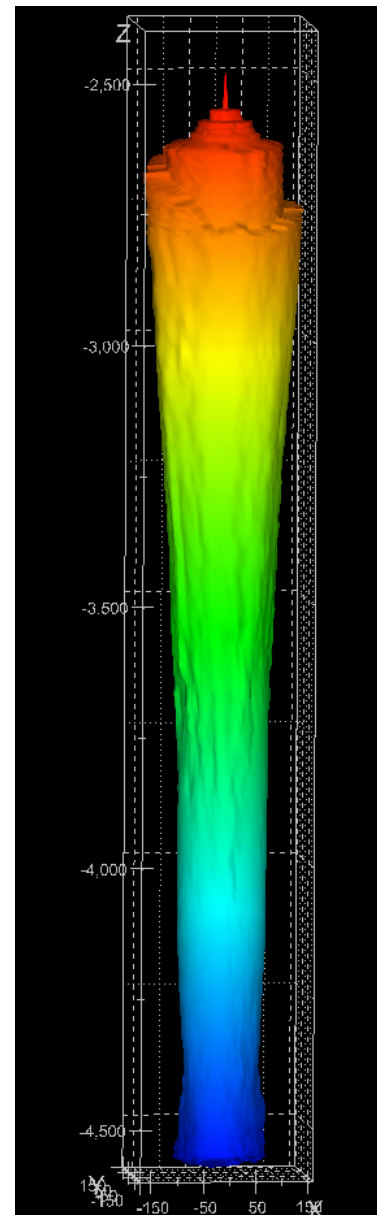


Figure 3-6: Image from the 2013 Sonar of WH117.

Table 3-5: Timeline of selected WH117 events, and logs.

Year	Event
1983	Well A completed (Franks 1984a)
1984	Well B completed (Franks 1984b)
1988	Leaching Completed
1989	MIT
1994	MIT
2004	MIT, Sonar
2009	MIT
2010	Multiarm Caliper Survey (Cassidy 2010)
2013	Sonar
2014	MIT (McCoy 2014)

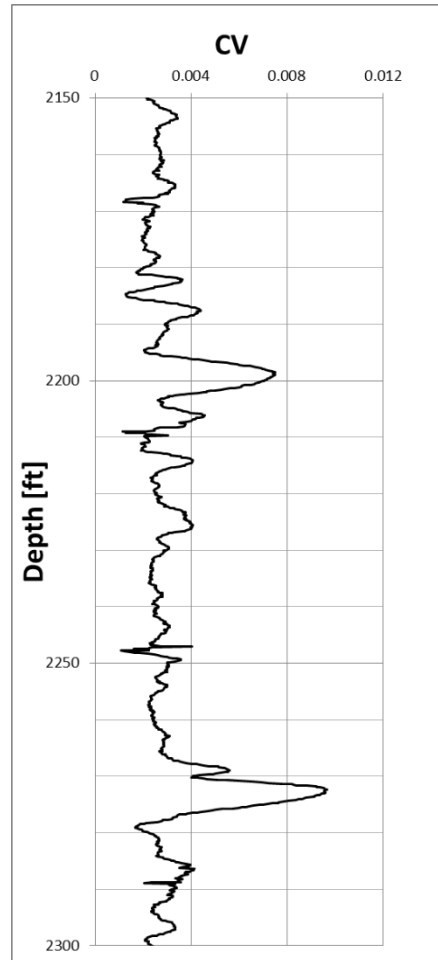


Figure 3-7: Coefficient of variation of the casing diameter obtained from the MultiArm Caliper (MAC) survey of July 2010. Image shows a zone of increased ovality around 2200 ft and 2275 ft.

4 Methodology

4.1 Hydrostatic Column Model

A numerical model was used to simulate the hydrostatic fluid pressure and density distributions in the cavern wells in order to provide a theoretical basis for analyzing the pressure relationships observed at the cavern wellheads during the test period.

4.1.1 Model Domain

Each well was modeled separately with a finite difference approach. Well internal diameters (ID) were estimated from nominal cemented casing diameters in the cased sections, and from a combination of nitrogen injection and sonar data in the salt chimney and cavern. The model was effectively 1-dimensional with depth (z), and fluid properties (pressure, density, temperature) did not vary in the horizontal direction across the diameter of the domain. Variable zone sizing (Δz) was used and zone sizes were refined over key depth zones where fluid interfaces (nitrogen-oil) occurred. A logical sketch of the model domain for a representative well is given in Figure 4-1.

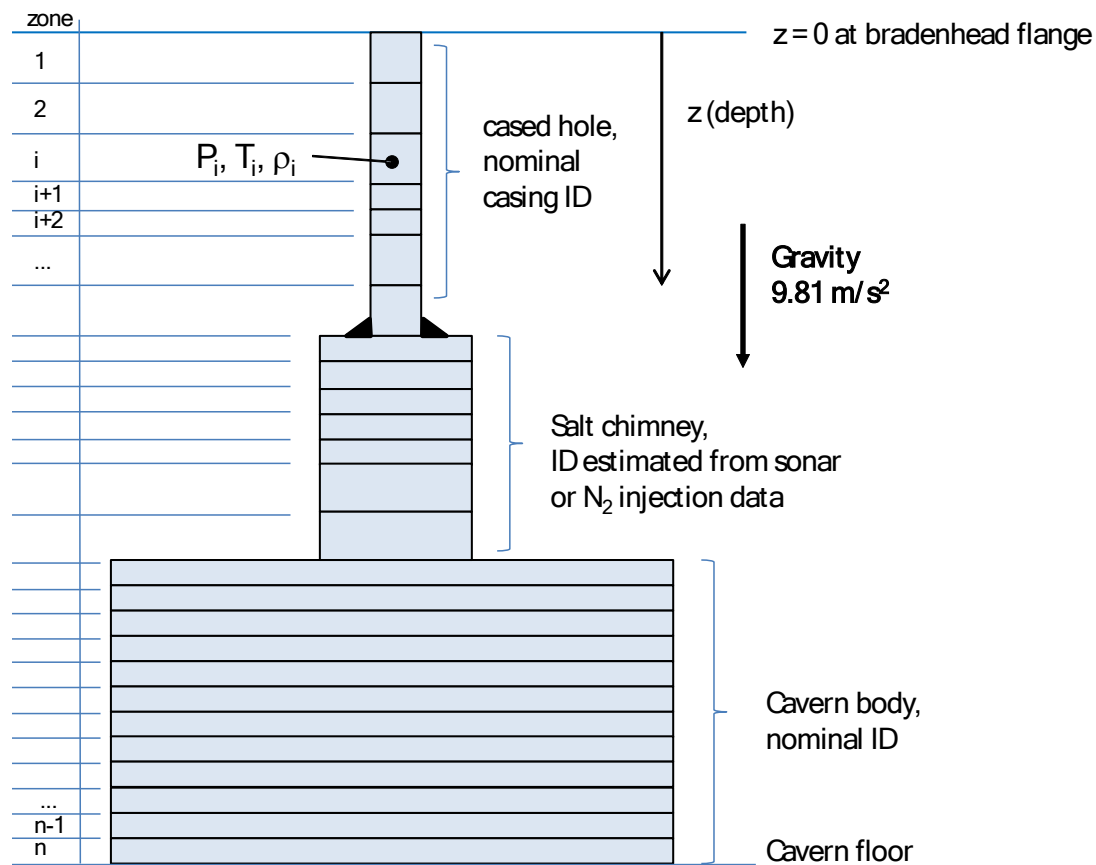


Figure 4-1: Logical diagram of computational mesh used in hydrostatic column model.

4.1.2 Fluid Pressure Model

Fluid pressures were calculated by incrementing with depth using a linear hydrostatic equation:

$$P_{i+1} = P_i + \rho_i g(z_{i+1} - z_i) \quad (3-1)$$

Where:

P = pressure
 ρ = fluid density (gas or liquid)
 g = gravitational acceleration
 z = depth

Subscript i = index for computational cell

Liquid density (ρ_i) was calculated using a linear correction from standard conditions to in-situ conditions:

$$\rho_i = \frac{\rho_o}{(1 - (P_i - P_o)E)(1 + \beta(T_i - T_o))} \quad (3-2)$$

Where:

T = Temperature
 ρ_o = density at standard pressure (P_o) and temperature (T_o)
 E = liquid bulk modulus of elasticity
 β = liquid thermal expansion coefficient

Gas density (ρ_i) was calculated using the ideal gas law model (Sonntag and Van Wylen 1991):

$$\rho_i = \frac{P_i}{RT_i Z} \quad (3-3)$$

Where:

R = gas constant (specific to nitrogen) = 296.8 [N m/Kg K]
 Z = ideal gas compressibility factor

Temperature varies with depth in a cavern well, typically increasing with the geothermal gradient in the narrow well section and then reaching a nearly constant value inside the cavern. For wells simulated in this report, temperature was determined by wireline measurement.

Wellhead pressure is typically measured with a pressure transmitter and serves as a starting point for the model. A small correction for depth offset from the measurement point to the zero depth point at the BHF is implemented in the model.

4.1.3 Predicting Nitrogen-Oil Interface Depths

One requirement of the model is to predict the nitrogen-oil phase interface depth. The approach used in the current discussion is to simulate two parallel, uncoupled columns of fluid with known wellhead pressures and find the depth at which the fluid pressures are equal. Graphical output from the model is shown in Figure 4-2. The model also calculates total mass of gas from BHF to

the interface depth and saves this value as a reference point for use in simulating the behavior of a completely gas-tight well.

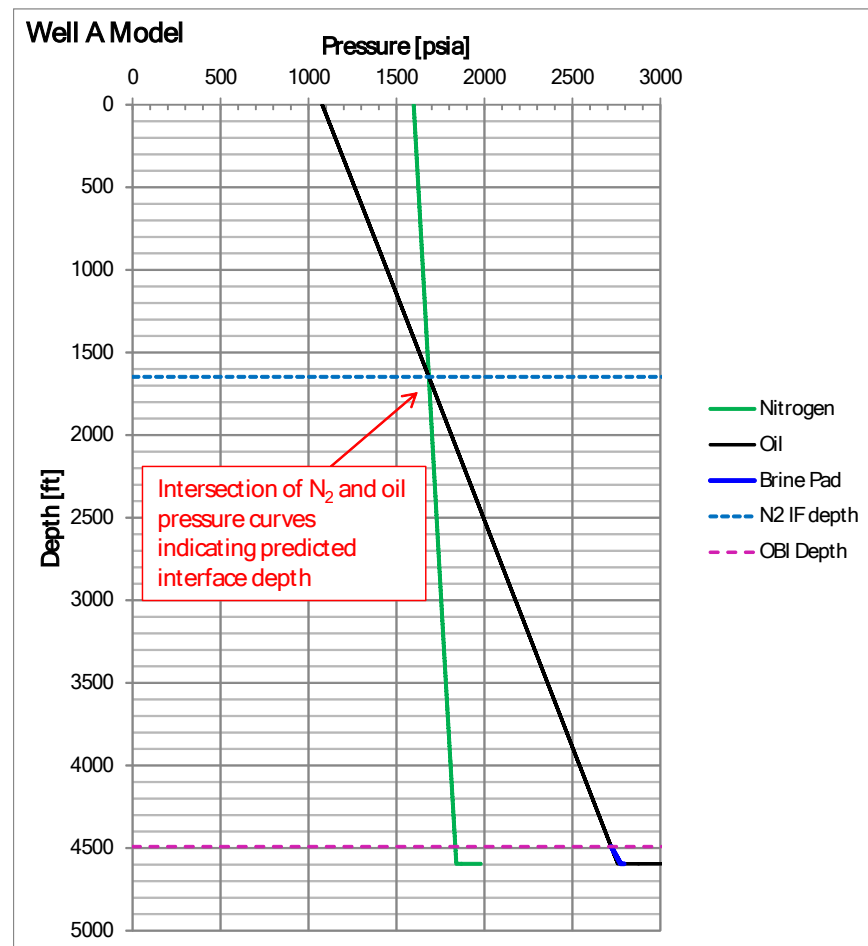


Figure 4-2: Graphical model output showing intersection of pressure curves indicating predicted N₂-Oil interface depth.

4.1.4 Predicting Pressure Change at the Gas Wellhead with Creep Closure

The model is also used to simulate the expected interface displacement and gas wellhead pressure after the cavern has experienced a pressure rise due to creep closure. This is a variation on the interface calculation described above. An overview of the process is given here.

- Typically, brine pressure observed at the wellhead with a hanging string is taken as input.
- For a gas-tight well the assumption of constant gas mass in the system is taken. On the other hand, the mass of nitrogen can be decremented in a controlled manner if a leak is modeled.
- The oil-brine interface (OBI) depth (typically in the body of the cavern) is taken to be a stationary reference point ($z = \text{constant}$) for calculations that do not involve liquid movement in or out of the cavern. For a typical SPR cavern with a nominal 200 ft. diameter, a movement of ~5,600 bbl liquid is required in order to move the interface 1

foot, so this constant interface assumption is reasonable for the simulations run in this report.

- To couple the brine string well with the nitrogen-capped one, we set the pressure at the end of tubing (EOT) depth to be identical in both wells. Creep-induced pressure increase is manually simulated in the model by adding small increments to the brine wellhead pressure. In order to maintain a pressure balance at EOT, the oil wellhead pressure is incremented accordingly, (normally the pressure will increment the same amount). The difference between calculated pressures at EOT is monitored for a minimum.
- The nitrogen well pressure along the whole nitrogen column is calculated with the condition of constant mass of nitrogen in the system (prior to incrementing the brine well pressure). The model is run manually to find a nitrogen wellhead pressure with the known nitrogen mass that intersects the oil well pressure curve; the point of intersection being the predicted NOI. In practice, the model monitors nitrogen mass above the intersection point and minimizes the difference between the starting condition mass and the ending condition mass.

4.2 Data Acquisition and Processing

4.2.1 Hourly Wellhead Pressure

The acquisition of pressure measurement at the wellheads was conducted in two ways:

- Hourly emails from DCS (Distributed Control System)
- SPR historian database.

A software utility was built to receive and process the hourly emails and the data was analyzed in a spreadsheet workbook. The various pressure channels are labeled as specified in the wellhead drawings (See Appendix WELL DRAWINGS) and shown in Table 4-1.

Table 4-1: Labels for pressure and temperature channel per well head drawings.

Wellhead drawing label	Data historian label	
PI41	3C117PI41PV	WH117A-oil
PI43	3C117PI43PV	WH117A-cem ann.
PI32	3C117PI32PV	WH117B-brine
PIC30	3C117PIC30PV	WH117B-oil
PI33	3C117PI33PV	WH117B-cem ann.
TI13	3C117TI13PV	WH 117 well pad

Additionally, temperature and high resolution pressure logs were carried out at test initialization (Mar 27, 2014) and finalization (Apr 24, 2014). The logs were carried out by E&P Wirelines Services.

4.2.2 Temperature Effect on Instrumentation

The effect of atmospheric temperature on the instrumentation and the wellhead equipment has also been taken into consideration. The wellheads do not have temperature sensors in them, but a single one is placed along the piping on the well pad. A schematic of the well pad instrumentation is contained in the appendix (WH117, Piping and Instrument Drawing, WH-M-103-127, 12/5/2011). The sensor measures the temperature of the fluid inside the pipe, which is exposed to the elements. We expect the measured temperature to closely follow the atmospheric one, which was confirmed by comparing the atmospheric temperature measured at the closest weather station. Both temperatures are shown in Figure 4-3, and even though the magnitude of the temperature at the well pad is higher, the local trend is closely followed.

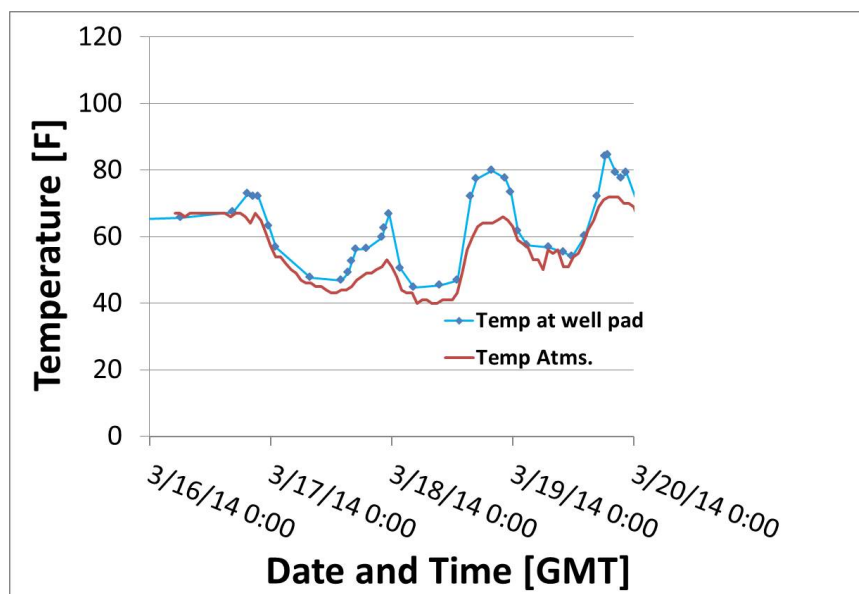


Figure 4-3: Temperature measured at the well pad for WH117 during the nitrogen testing. Included in the figure are the atmospheric temperature observed at Lake Charles regional Airport, LA. <http://www.friendlyforecast.com>.

4.2.3 Wireline Data

Wireline logs at selected times early and late in cavern pressurization cycles were obtained by running a set of wireline tools downhole through both the slick well and hanging string well to collect continuous fluid property profiles (temperature, pressure) with depth. A picture of a wireline tool, showing the geometry of the temperature probe, is shown in Figure 4-4. The logging data were collected by the wireline operator and compiled and presented in tabular and graphical format presented in digital (PDF and LAS) data files. Data files were transferred to FFPO who forwarded them to Sandia.

The wireline tools were run from the wellhead to the bottom of the cavern in order to measure the complete temperature and pressure profile in each well, and find the nitrogen-oil interface in both the slick and hanging string wells. The focus of the test is on the fluid properties (temperature, pressure) within each well. Data inside the cavern body were also of interest, but

to a lesser extent than in the well. Hence, when optimizing the test configuration, most effort was directed at collecting data in the region between the BHF and cavern roof.



Figure 4-4: Wireline tool used to collect fluid properties during logging operation with temperature probe indicated.

4.2.3.1 Tool Specifications

The wireline tools used met specifications for use in SPR caverns, which included the ability to pass through the SPR wellhead and cased slick hole for the WH117A-well, nominally 12.5 in ID, or through the hanger and suspended casing for the WH117B well, nominally 9.85 in ID.

Additionally, the expected cavern temperatures range is about 80-130°F, with absolute pressures ranging from about 300-2500 psia. Below are the log tool specifications as requested prior to the long term Nitrogen test:

Temperature. Temperature accuracy to ± 2 °F will be adequate. Resolution should be equal to or better than 0.1 °F. The Lee Specialties Pressure/Temperature/Flow (PTF) Sensor tool (**Error! Reference source not found.**) offered by Schlumberger E&P Wireline meets these specifications.

Pressure. Pressure accuracy to ± 2 psi will be adequate. Resolution should be equal to or better than 0.02 psi. High resolution in pressure is very important for calculating the pressure gradient, which is computed from relative pressure differences with depth. The Lee Specialties Pressure/Temperature/Flow (PTF) Sensor tool (**Error! Reference source not found.**) offered by Schlumberger E&P Wireline meets these specifications.

Interface. The nitrogen-oil interface and oil-brine interface depths must be determined within ± 0.5 ft. for both the slick well and the static annulus. While the high-resolution pressure tool

should find the phase interfaces in the slick well, it will not find the interface in the static annulus while the tool is hanging inside the brine string. A gamma ray tool or similar will be needed to locate the interface in the static annulus.

4.2.3.2 Timing of Wireline Surveys

The fact that MIT was run on this cavern in the months preceding the test gave some good baseline data on well temperature and interface locations. An initial Casing Collar locator (CCL)/gamma density wireline survey was run in the A-well on Mar 13, 2014 after some nitrogen was bled off in order to re-position the NOI from the MIT position at 2422 ft to the starting position for the special test at 1655 ft. Combined wirelines (high resolution pressure, temperature, gamma, CCL) were also run on Mar 27, 2014 in order to initialize the special test, and on Apr 23, 2014 in order to finalize the test. A schematic of the tool stack used to support this analysis is given in Figure 4-5.

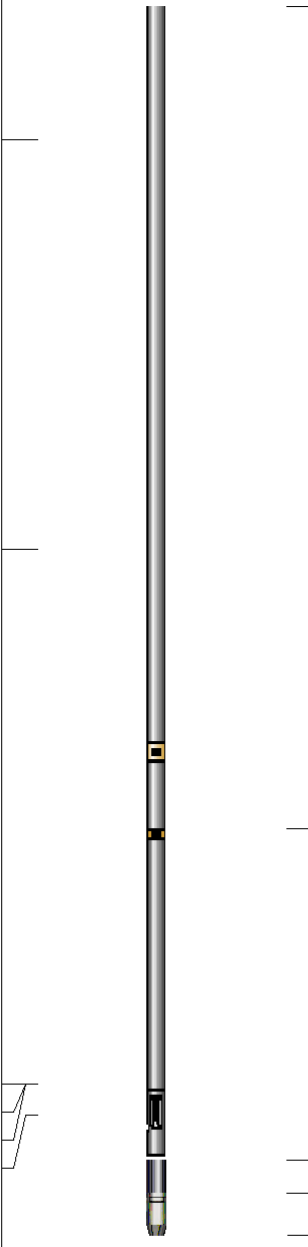
Sensor	Offset (ft)	Schematic	Description	Len (ft)	OD (in)	Wt (lb)
CCL	6.62		LTELGR-A (0411-068) LEE TELEMETRY GAMMA RAY	4.97	1.38	
GR	4.14					
			LeePT-LEE (1102-1587) Lee Pressure Temperature Tool	2.00	1.38	5.00
PTEMP	0.91					
PRESS	0.91					
PTEMP	0.91		spacer 1 3/8" SOURCE SPACER	0.20	1.38	3.00
TEMP	0.72		source CS 137 SOURCE	0.25	1.38	1.00
		Dataset:	wh117b23apr14.db: field/well/run1/pass5			
		Total Length:	7.42 ft			
		Total Weight:	9.00 lb			
		O.D.	1.38 in			

Figure 4-5. Schematic of the combined wireline tool run at special test initialization (Mar 27, 2014) and finalization (Apr 23, 2014) on WH117A and B.

4.3 Nitrogen Test Configuration

The extended nitrogen test described in this report was run after the January 2014 MIT and before the nitrogen was completely bled off the wells. The A-well nitrogen-oil interface position was moved from its MIT depth of ~2424 ft. (just below the casing shoe) up to 1646 ft. which is inside the steel casing with a well internal diameter of about 1 ft. The B-well nitrogen-oil interface position was placed at ~2419 ft. in the salt chimney just below the casing shoe in both the MIT and the extended nitrogen test, where the well internal diameter is about 4 ft. A conceptual sketch of the test configuration is shown in Figure 4-6. Depth datum in all cases is the BHF.

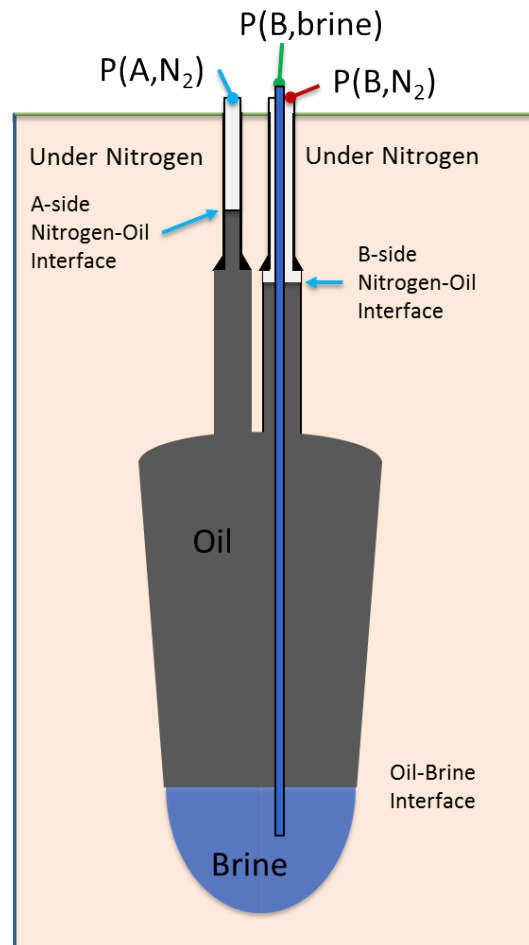


Figure 4-6. Conceptual sketch of the cavern during the extended nitrogen test. Note A-side NOI is inside the casing (ID ~ 1 ft), while the B-side NOI is in the salt chimney (ID ~ 4 ft).

5 Analysis of Cavern Monitoring

A number of monitoring tools were utilized to fully understand the condition of WH117 cavern and its wells:

- Pressure monitoring at the wellheads as well as annuli
- Pressure of neighboring caverns
- Previous logs from Jan 2014 MIT
- High resolution P, T logs

5.1 Wellhead Pressure Data

Both WH117 wells were held under nitrogen from Dec 2013 through May 2014. A glance at the pressure history at the wellheads for the past 6 months is shown in Figure 5-1.

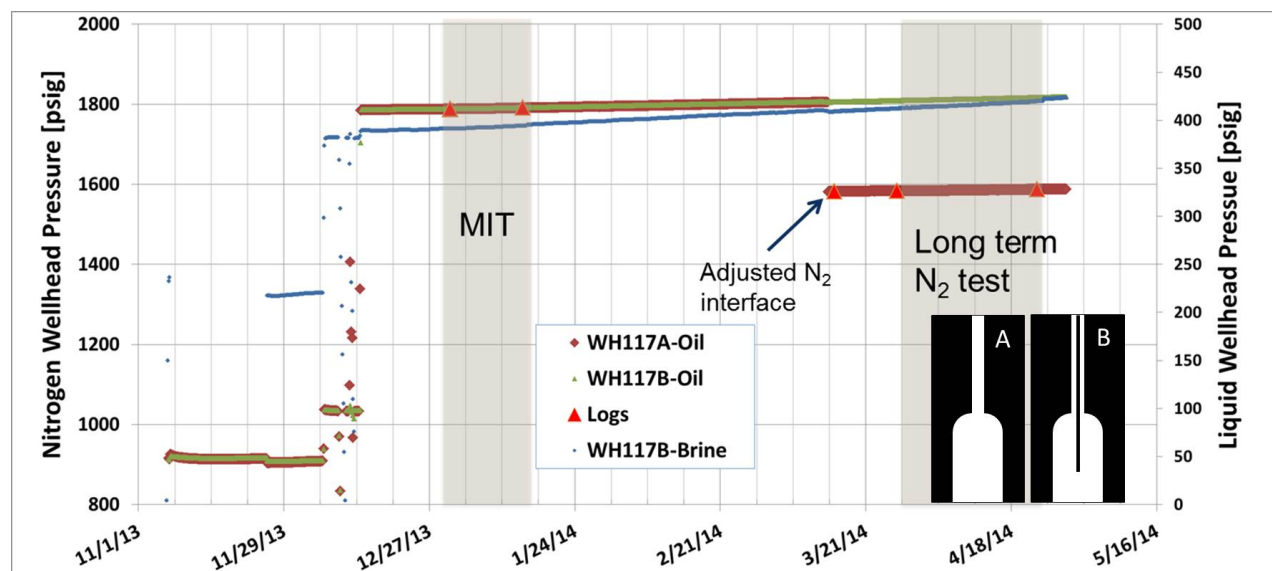


Figure 5-1: Wellhead pressure history for cavern WH117 from Nov. 2013 to May 2014.

The cavern underwent its regularly scheduled MIT (every 5 years) in Jan 2014. In preparation for the test, nitrogen was injected in both well A and B on Dec 14, 2013. The initialization and finalization log for the MIT were run in Dec 3, 2013 and Jan 14, 2014 respectively, and the cavern passed the MIT. Pressures were held for a length of time in preparation for the long term nitrogen monitoring test. On March 13, 2014 nitrogen was bled from well A to move the interface around 1650 ft in order to match more closely the conditions of the Big Hill wells. Well B NOI was left at 2419 ft, same as the MIT (see Figure 4-6 for conceptual illustration of interface positions).

The wellhead pressures were carefully monitored during the long-term test which started on Mar 27 and ended on Apr 23. Figure 5-2 shows the hourly wellhead pressures for well A during this test. The pressure of the brine string in well B is also shown, taken as the representative pressure of the liquid in the cavern. A linear fit to the pressure data for well A found an average pressure rate of 0.169 psi/day, which is 0.59 times the pressurization of the brine string.

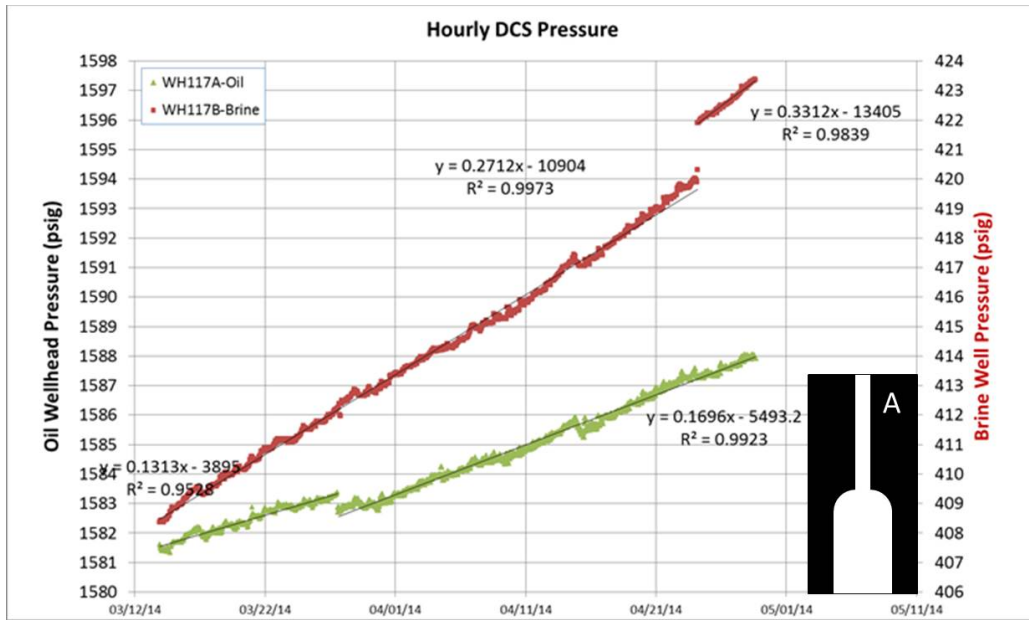


Figure 5-2: Wellhead pressure for WH117A under long-term nitrogen monitoring.

The pressure data for WH117B is shown in Figure 5-3, and it is found to have a pressurization rate of around 0.28 psi/day, very close to the brine string pressurization rate. After close analysis of the data, we note that the pressure slope is slowly varying, and in fact toward the end of the test we find very different ratios. For example, Figure 5-4 shows the wellheads pressures for well A and B as they compare to the brine pressure. The vertical dashed lines bound the date range over which the pressure rate was calculated. For this interval the rates are included in Table 5-1, and differ from the rates averaged over the full duration of the test.

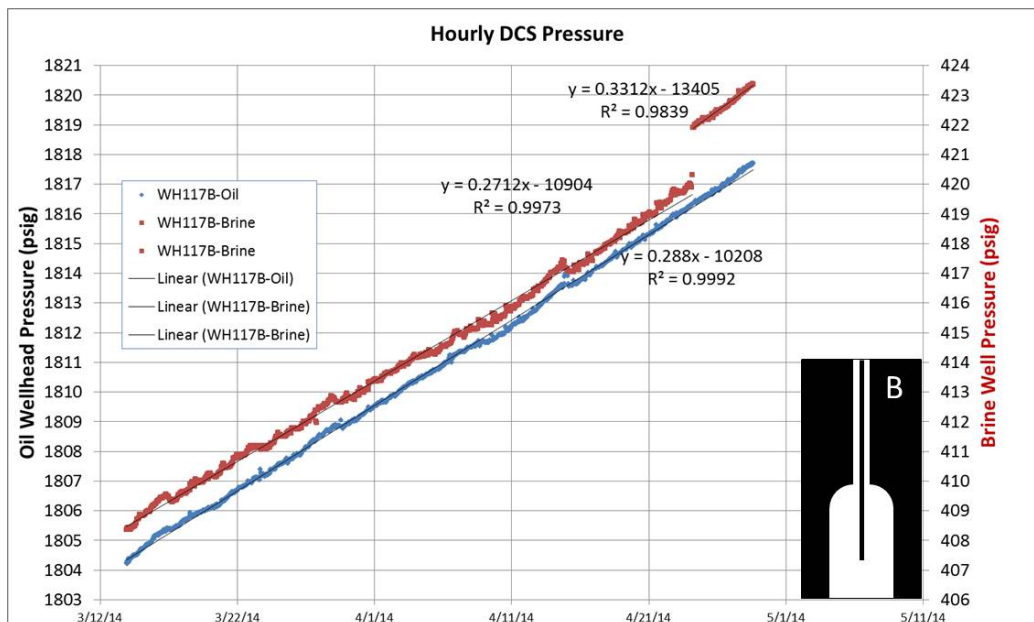


Figure 5-3: Wellhead pressure for WH117B under long-term nitrogen monitoring.

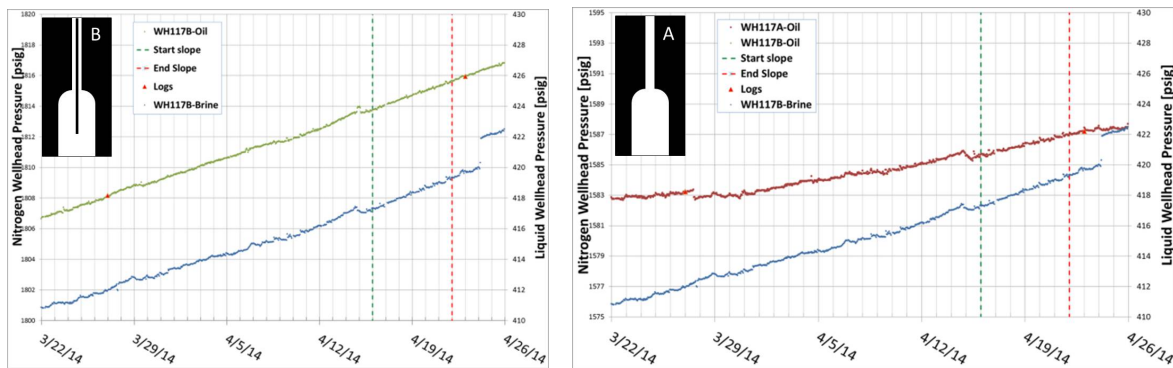


Figure 5-4. Illustration of pressurization rates for WH117A (right) and 117B (left). The vertical lines bound the data that has been fit for comparison.

Table 5-1: Pressurization rates relative to brine calculated between April 16-22, 2014.

			WH117B-Brine	WH117A-Oil	WH117B-Oil
Start Date	4/16/2014	Slope (psi/day)	0.342	0.233	0.310
End Date	4/22/2014	Rs _q	0.988	0.969	0.994
		Relative Slope	1.00	0.68	0.90

One of the things that can affect the slope calculation is measurement noise that is not directly related to the pressure in the cavern, but to instrumentation. For example, the dip in pressure around April 14, was found to be related to a local cold front. Figure 5-5 shows the wellhead pressure for well A during the nitrogen testing and the correspondent temperature as measured at the well pad. As discussed in section 4.2.2 the fluid temperature measured at the well pad tracks the ambient temperature. From this figure we can track the drop in the wellhead pressure to a downturn of the ambient temperature.

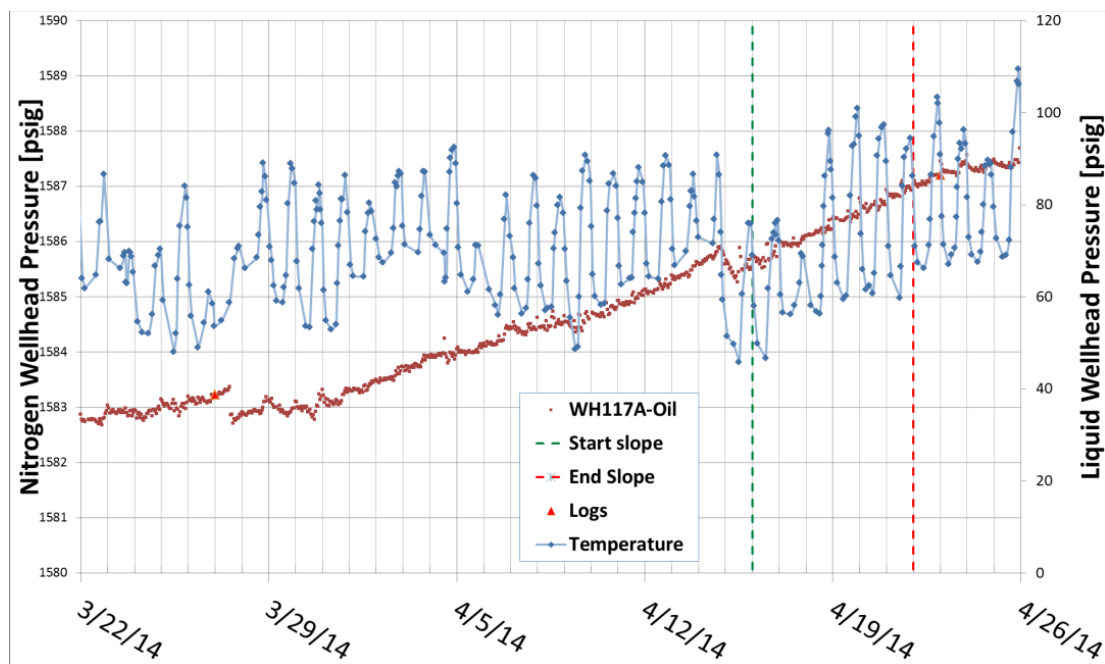


Figure 5-5: Well head pressure of WH117A superimposed on temperature data also measured at the well head.

Taking environmental factors into consideration, we obtained an estimate for variations in the pressurization rates by repeating the slope calculation at different time intervals (eliminating the time around the cold front) and we found them to be between 0.58-0.68 for well A and 0.90-1.0 for well B.

5.1.1 Cemented Annulus Pressures

The presence of pressure in the cemented annulus that is responsive to product pressure indicates integrity issues related to primary product containment (also discussed above in section 3.1). To some extent, pressure in the cemented annulus could be ascribed to elastic expansion and contraction of the product string, though this is limited in magnitude and should be very fast and reversible. Pressure due to hydraulic leaks may show a range of response times and are not always immediately reversible. Fluid pressure can communicate from the product side to the cemented annulus through a leaky casing shoe, threaded couplings, holes from deformation or chemical attack, or even seals at the wellhead. Analyzing the relationship between the pressure inside the wellbore and the annulus can indicate what type of hydraulic connection exist and can be a precursor to a leak that is not yet obvious from the wellhead pressure measurements.

5.1.1.1 BM4-B Example

An example of complete hydraulic connection for SPR well BM-4B is shown in Figure 5-6, where the annulus pressure quickly follows any changes in the wellbore pressure.

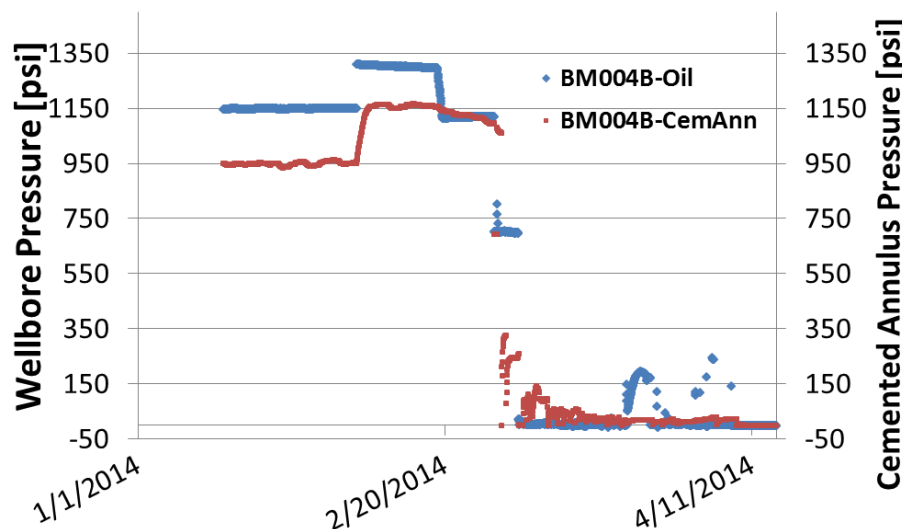


Figure 5-6: Wellbore pressure as it compares to the cemented annulus pressure for BM004B.

5.1.1.2 WH117 A,B cemented annulus

Switching focus back on WH117, the pressure in the cemented annulus for both well A and B were monitored for the period Nov. 2013 through May 2014. As shown in Figure 5-7, there appears to be no fluid pressure build up in the cemented annulus of well A. Note the pressure scales on the left and right axes differ by three orders of magnitude. Despite the large variation in the product side well pressure, especially during nitrogen injection on Dec 2013 and pressure drop in March 2014, the cemented annulus seems to have no response to its internal pressure. A similar behavior is shown in Figure 5-8 for well B. From the analysis of the pressure in the annulus we can conclude that there seem to be no apparent hydraulic connection between the inside of the casing and the cemented annulus for both wells in this cavern. One caveat is that the monitoring point on the cemented annulus is at the ground surface near the BHF, and it is possible that the monitoring point is isolated from other areas within the cemented annulus that are pressurized.

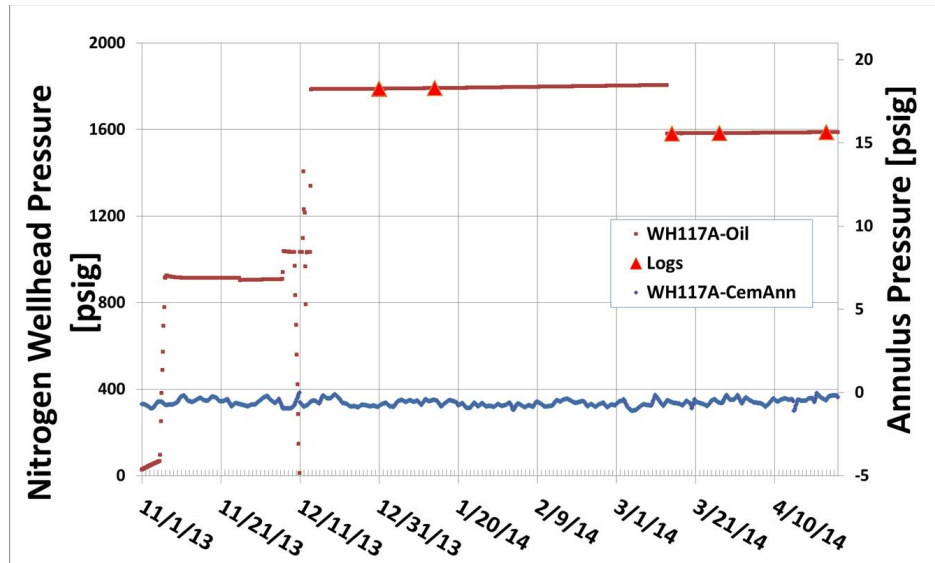


Figure 5-7: Pressure of the cemented annulus in well WH117A for the past six months as they compared to the pressure inside the casing.

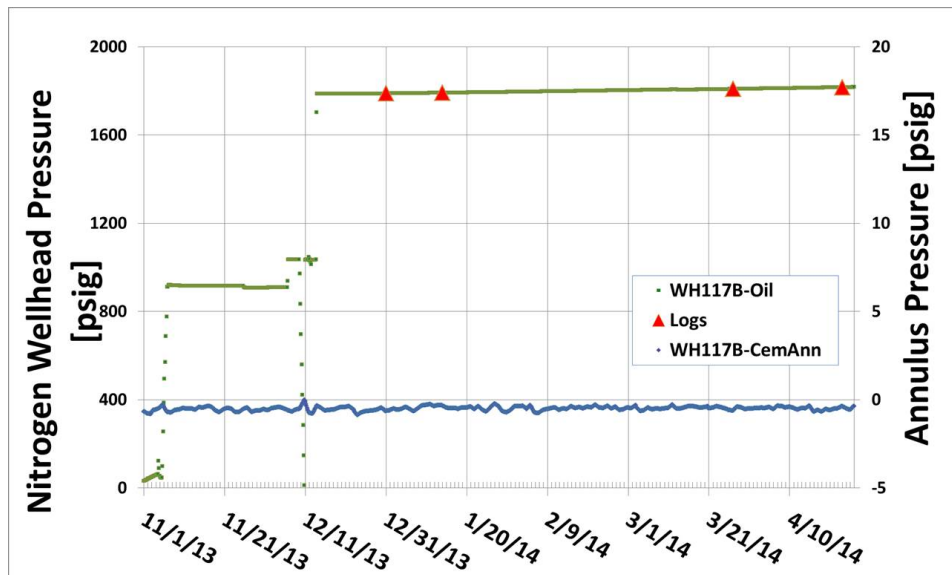


Figure 5-8 Pressure of the cemented annulus in well WH117B for the past six months compared to the pressure inside the casing.

5.1.2 Neighbor Cavern Activity

It is well known that the salt creep properties are highly non-linear and the creep rate is highly depended on the stress field. In practice, this means that fluid pressure in the neighboring caverns can have measurable effect on the stress in the formation and therefore the closing rate of a cavern. It is useful to look at the activity in neighboring caverns of WH117 during the duration of the test to check if any ‘out of ordinary’ pressure behavior is seen, most importantly to include rapid changes in pressure associated with workovers. The caverns considered are WH105, WH106, WH108, WH11 and their locations shown in Figure 5-9. Note also that the wellhead of WH117 was de-piped during the test and therefore no pressure communication was possible though surface piping.

The neighboring caverns were not found to be depressurized, but mostly in within their normal operating ranges, shown in Figure 5-10. Cavern 106 pressures do change erratically during period, but this was due to fluid injection/removal from the SPR ‘Cavern Capacity Maintenance Program’ which was actively leaching on site. Pressure changes of this magnitude have not been observed to affect measurable changes in neighbor pressurization rates in the past.

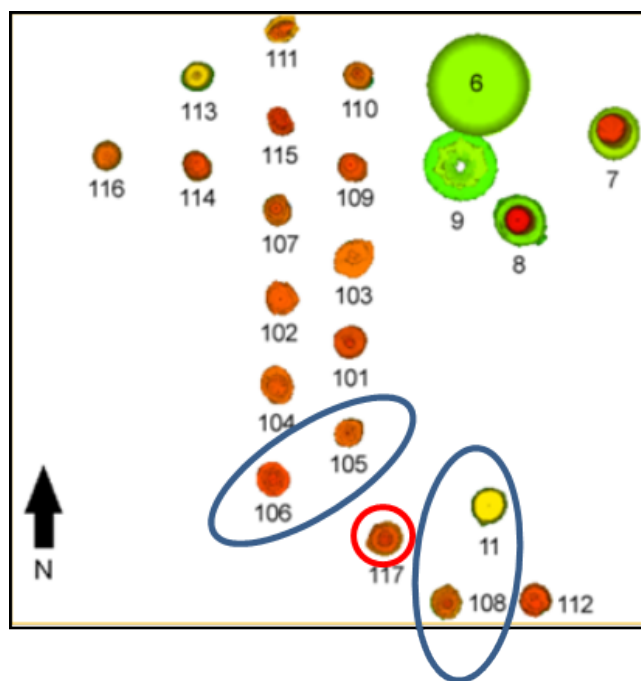


Figure 5-9: Subsurface plan view of West hackberry cavern field. WH117 is circled in red, and nearest neighbor caverns are circled in blue.

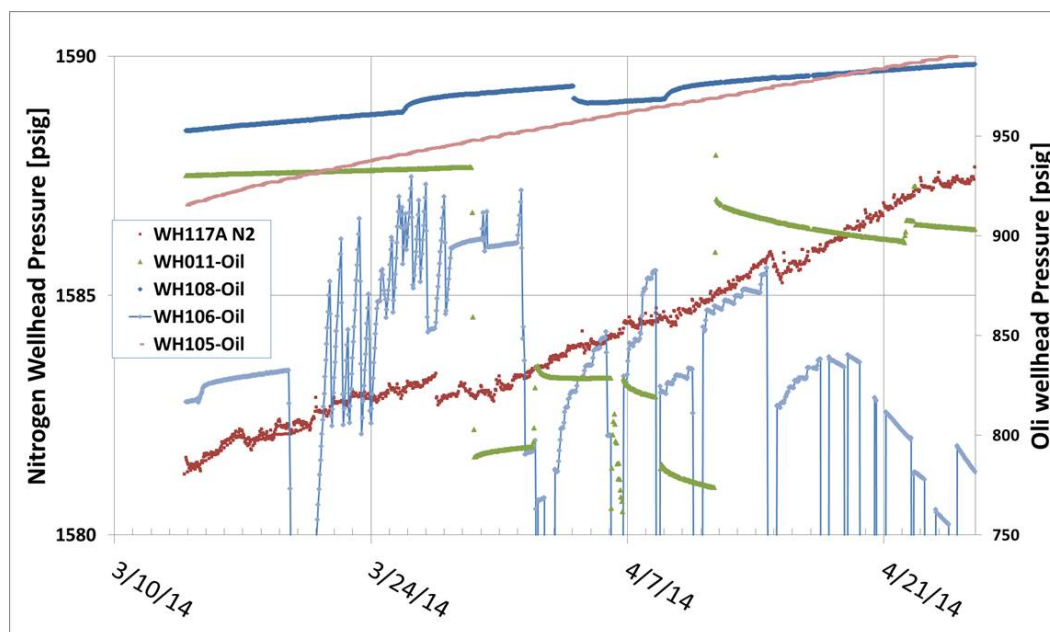


Figure 5-10: Pressure history of WH117 neighboring caverns during the nitrogen test.

5.2 2014 MIT on WH117

A state-required MIT was conducted in cavern 117 in Jan 2014. Nitrogen was injected on Dec 13, 2013 and the test was conducted between Dec 31, 2013 and Jan 14, 2014. Table 5-2 summarizes the wellhead pressures and the NOI of the MIT test. The test passed and the cavern deemed tight. The MDLR for WH117A was calculated to be 23.5 bbl/yr and a leak rate of 1.3 bbl/yr was found. Similarly for WH117B a MDLR of 26.1 bbl/yr was calculated with a leak rate of 2.2 bbl/yr. A final report was filed on Feb. 2014 (McCoy 2014). Figures of the temperature logs are included in the appendix.

	MIT Well A Initial	MIT Well A Final	MIT Well B Initial	MIT Well B Final
Date of log	Dec. 31, 2013	Jan. 14, 2014	Dec. 31, 2013	Jan. 14, 2014
P(N₂) [psia]	1788	1791	1788	1791
P(brine) [psia]			391	394.5
NOI [ft]	2425	2424	2419	2418.5

Table 5-2: Summary of results from MIT logs.

5.3 Long Term Nitrogen Monitoring Test Logs

The long-term nitrogen monitoring test was run according to the specifications set in the test plan. Criteria for initialization and finalization were also included in the plan and allowed for equilibration time before the test was run. Initiation and finalization logs were run in both wells and are used to determine the NOI, as well as to look at the temperature and pressure distribution

as a function of depth. Table 5-3 lists some of the reported log results. The purpose of these logs is to calibrate the hydrostatic model with real temperature data, and to validate the results, NOI and pressure, as predicted by the model.

	Well A Initial	Well A Final		Well B Initial	Well B Final	
Date of log	March 27, 2014	April 23, 2014	Delta	March 27, 2014	April 23, 2014	Delta
P(N2) [psi]	1583	1587	5 psi	1809	1816	7 psi
P(brine) [psi]				412	420	8 psi
NOI [ft]	1646	1632	14 ft	2419	2419	0 ft

Table 5-3: Pressures and NOI of the long-term nitrogen monitoring test at initialization and finalization as reported by the logs.

5.3.1 Interface Depth Interpretation from Logs

The location of the NOI and OBI in well A was interpreted by analyzing the high resolution pressure log. The gradient of the pressure is expected to change abruptly across the interface due to the variation in density, which is shown as a kink in the pressure curve. This is illustrated in Figure 5-11, from which the measurement of NOI was taken to be 1649 ft. Similarly the NOI at finalization was taken to be 1636 ft. The OBI was confirmed to be constant across the two logs and was taken to be 4496 ft.

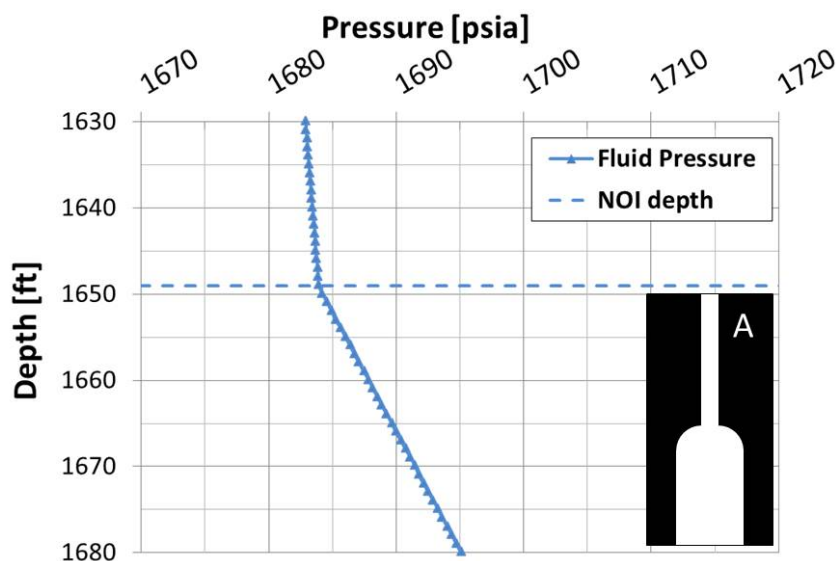


Figure 5-11: High resolution pressure log for WH117A around the expected NOI depth. Log conducted on Mar 27, 2014.

5.3.2 Well A Logs

Figure 5-12 displays the results from the initialization and finalization logs for well A. The pressure and temperature data is extracted directly from the log, while the fluid density is calculated from the derivative of the pressure with depth. The NOI is clearly visible from the change in slope of the pressure gradient, and therefore the large fluid density jump.

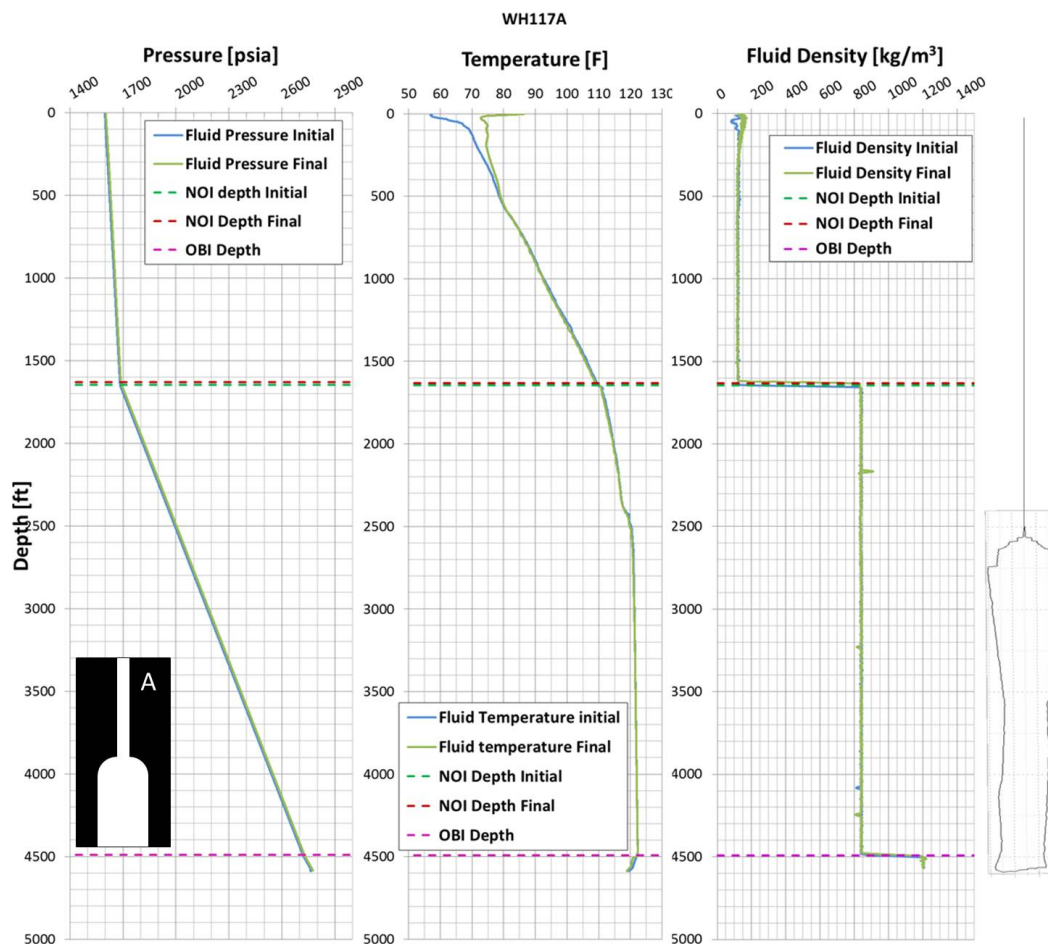


Figure 5-12: Logs results for WH117A. Initialization log ran on March 27, 2014, finalization on April 23, 2014.

A closer view of the pressure log (Figure 5-13) illustrates the pressure raise during the 4 weeks test period and the sharp change in pressure slopes corresponding to the NOI. The dashed lines correspond to the NOI depths, as taken by the method described in the previous section. A closer view of the pressure around the OBI, Figure 5-13 (right), shows how both logs, initial and final, place the interface 4492 ft.

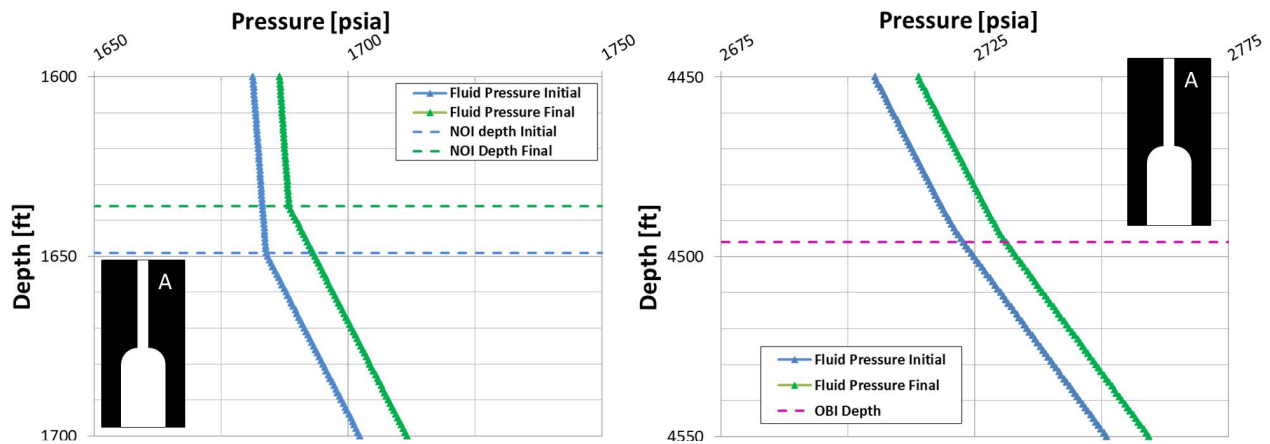


Figure 5-13: WH17A close up view of pressure log results highlighting the NOI movement during the test

As mentioned previously, the temperature logs are used as input to the model, but they can also reveal a number of important facts. The initial and final temperature logs are relatively consistent inside the cavern and the lower part of the well, but a large difference is shown in the first 500 ft below the surface, see Figure 5-14. This is likely related to the ambient temperature, which was 55°F in Mar 27 at the time of the log while it was 79°F on Apr 24th (<http://www.friendlyforecast.com>). The initial response (fast) of the temperature log is thought to be related to the temperature of the instrument, which is in equilibrium with atmospheric right before the test. The variation in temperature after the initial jump is, on the other hand, interpreted as the real temperature of the nitrogen column in the well.

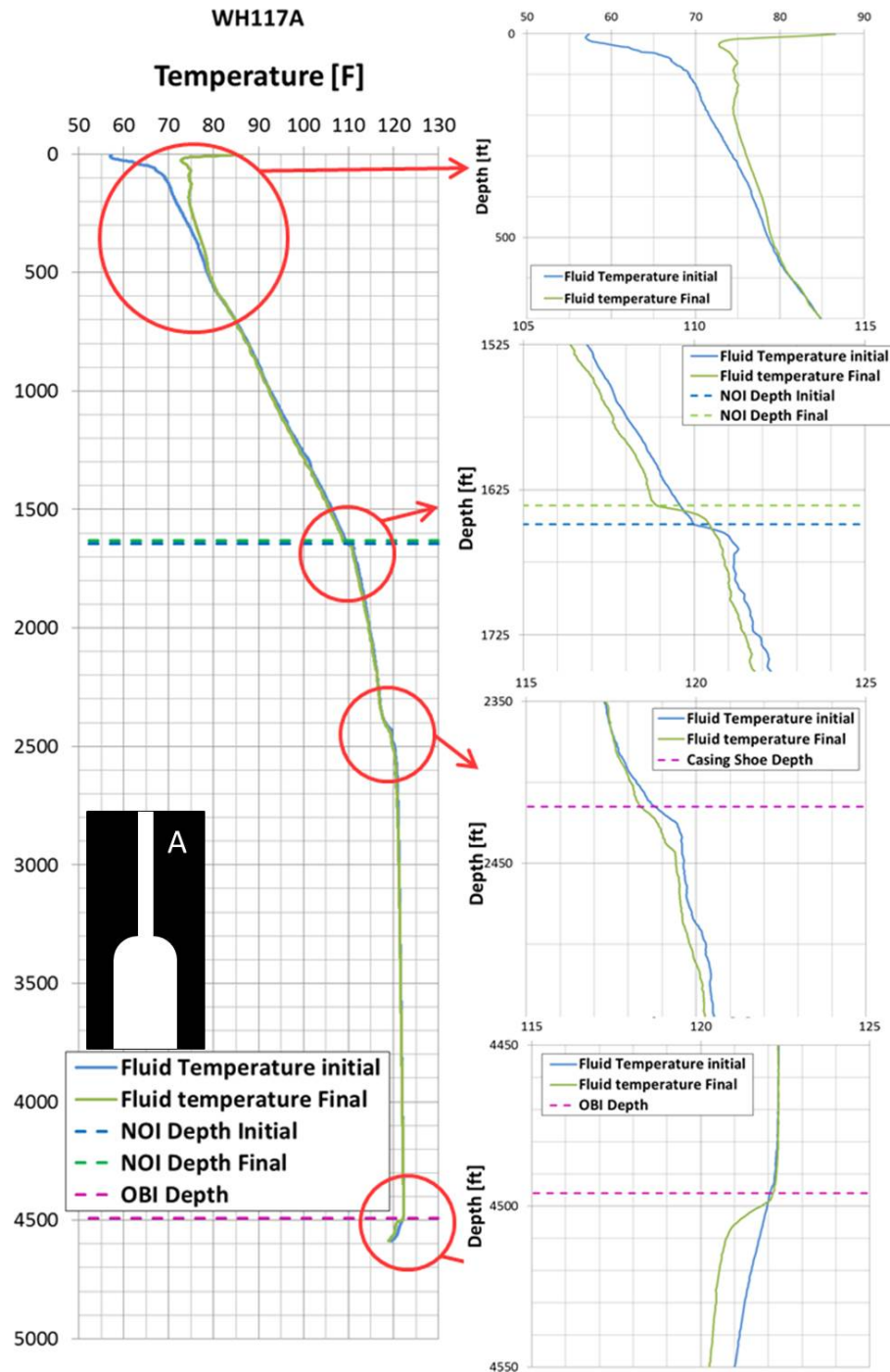


Figure 5-14: Close up view of WH117A Temperature logs for long term nitrogen monitoring test.

5.3.3 Well B Logs

The logs for the B well were acquired inside the brine string, which extends to 4565ft. An overview of the results is shown in Figure 5-15. Since the string is filled with brine, no pressure slope changes are seen at the NOI or at the OBI which are on the outside of the string. As expected the pressure gradient in the string remain relatively constant all the way down to the EOT. A detailed view of the temperature log is shown (Figure 5-16) for completeness.

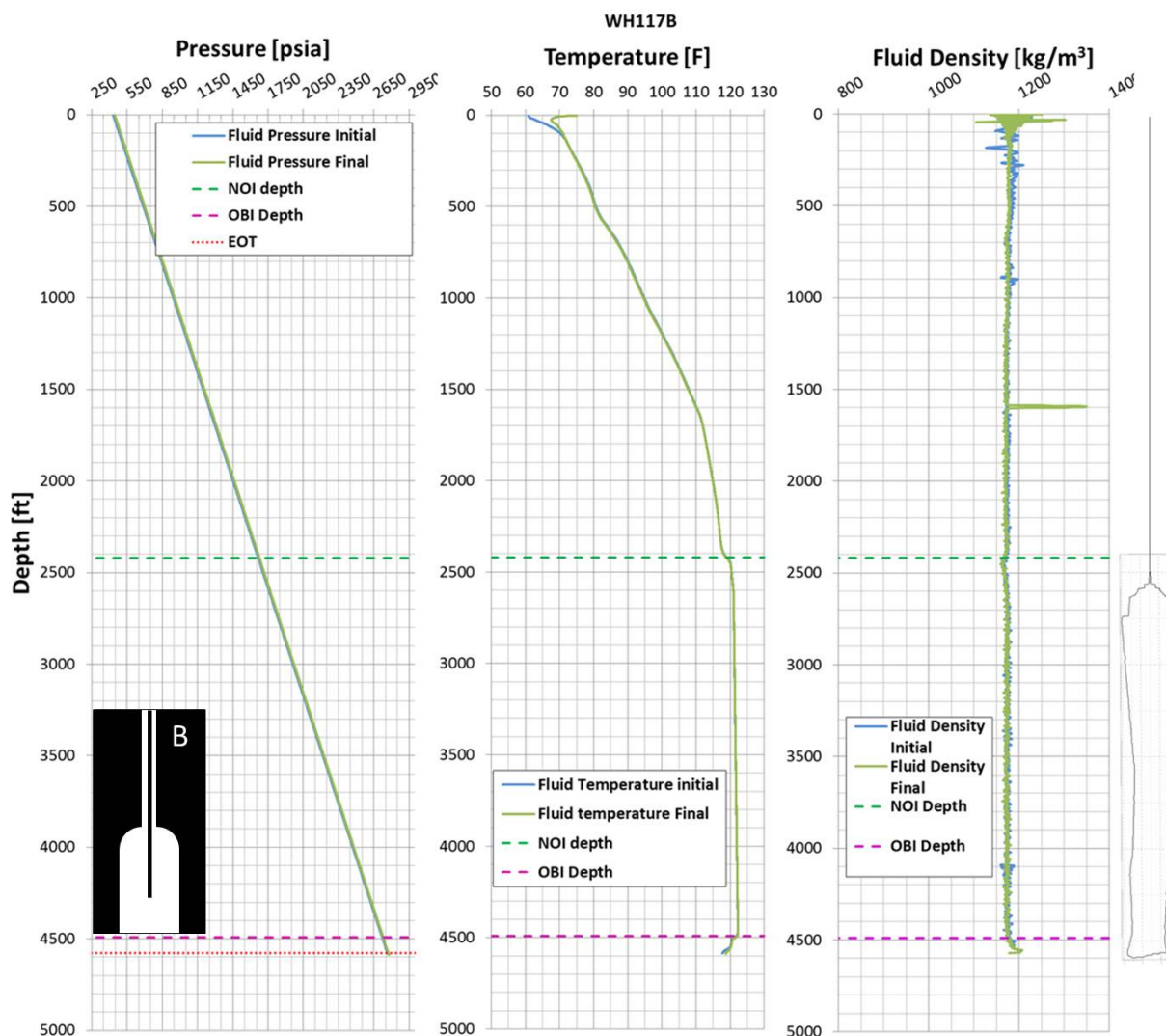
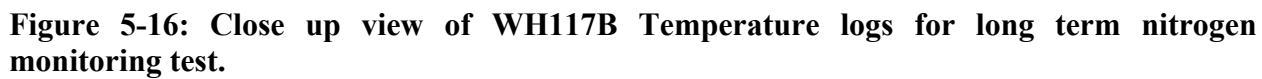


Figure 5-15: Logs results for WH117B. Initialization log ran on Mar 27, 2014, finalization on Apr 23, 2014.



6 Hydrostatic Column Model Results

6.1 Model Parameters

A list of the parameters used in the predictive model and their values is included in Table 6-1.

Table 6-1: List of parameters used in the hydrostatic column model

	Symbol	Value	Units	Description
oil	β	4.44E-04	1/F	liquid thermal expansion coefficient
	E	2.00E+05	psi	liquid bulk modulus of elasticity
	ρ_o	853	kg/m ³	density at standard pressure (P_o) and temperature (T_o)
Unsaturated Brine	β	1.15E-04	1/F	liquid thermal expansion coefficient
	E	3.10E+05	psi	liquid bulk modulus of elasticity
	ρ_o	1176	kg/m ³	density at standard pressure (P_o) and temperature (T_o)
Brine	β	1.15E-04	1/F	liquid thermal expansion coefficient
	E	3.10E+05	psi	liquid bulk modulus of elasticity
	ρ_o	1200	kg/m ³	density at standard pressure (P_o) and temperature (T_o)
Gas	P_o	14.7	psi	Pressure at standard conditions
	T_o	60	F	Temperature at standard conditions
	R	296.8	m·N/kg·K	gas constant (specific to nitrogen)(Sonntag and Van Wylen 1991)
	Z	1.04		ideal gas compressibility factor

The fluid densities computed in the model were compared to log measurements as shown in Figure 6-1. Each parameter (β , E , ρ_o , Z) was optimized to minimize the difference between modeled and measured pressure as shown in Figure 6-2. The brine pool at the bottom of the cavern was taken to be saturated brine, while the brine in the string was unsaturated. Additionally the density of the oil was compared to the SPR crude oil quality measurements data (included in the appendix) and found to match closely to their reported value. Well geometries (internal radius vs. depth) were determined from the West Hackberry cavern engineer's nitrogen injection workbooks (McCoy 2014). Adaptations of these for input to the hydrostatic column model are reproduced in Appendix: Model Well Geometry.

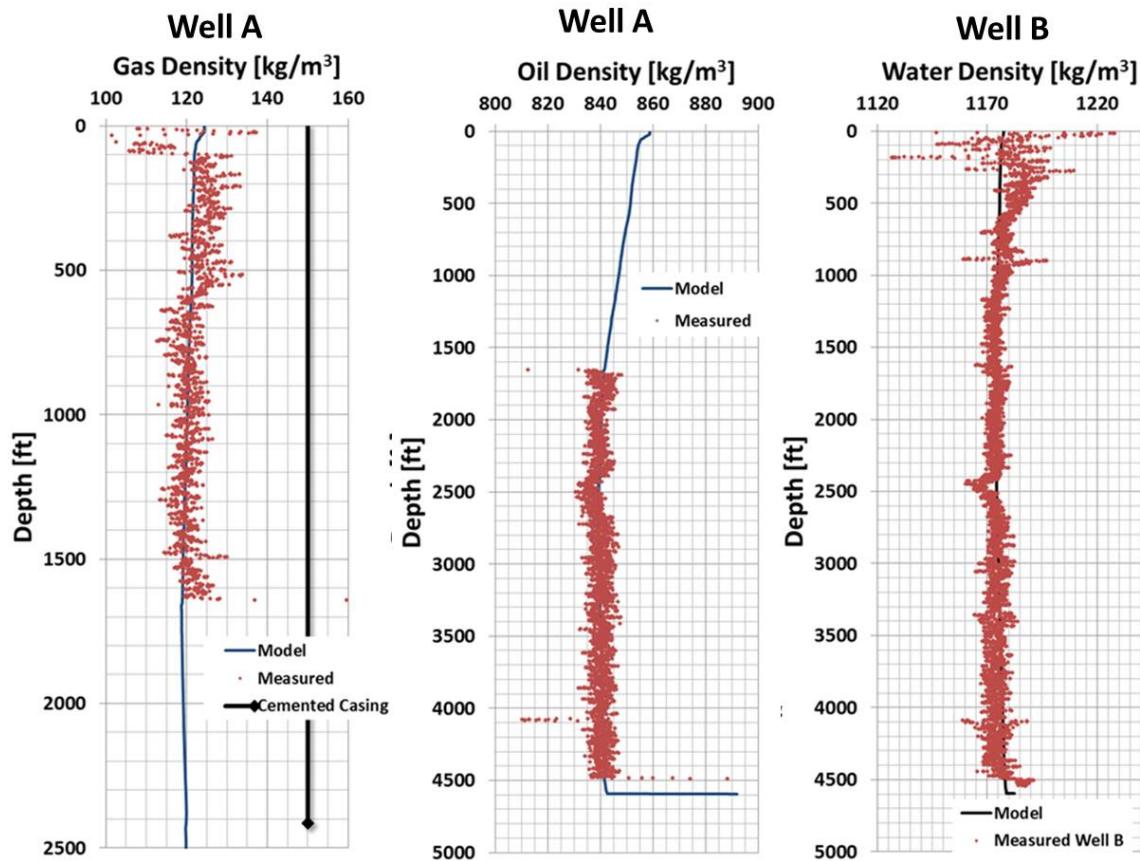


Figure 6-1: Fluid density calculated in the hydrostatic model as it compared to logging data from March 2014.

6.2 Model Predictions

The nitrogen column model described in section 4.1 was used to predict the pressurization rates as well as the location of NOI as a function of time. The wireline pressures were used to zero the model to the initial condition of the cavern and the initialization temperature logs are used as input to the model to calculate the fluid properties as a function of depth.

Figure 6-2 shows the difference between the pressure data from the initialization log and the model predicted pressures as a function of depth for well 117A. The two values match extremely well with the exception of a 2 psi offset below the NOI. The model is effectively predicting a NOI several feet deeper than observed. The reason for this offset is still unknown but it could be related to the magnitude of one of the model parameters, uncertainties associated with the measured data, or a breakdown of the hydrostatic assumption in the top ~500 feet of the domain where the temperature gradient is strongest and may be creating some localized natural convection. An in-depth model analysis and verification is planned for the near future. None the less the fact that the two sets of data match so closely gives us confidence that the model has been able to adequately capture the physics of the problem for the current application.

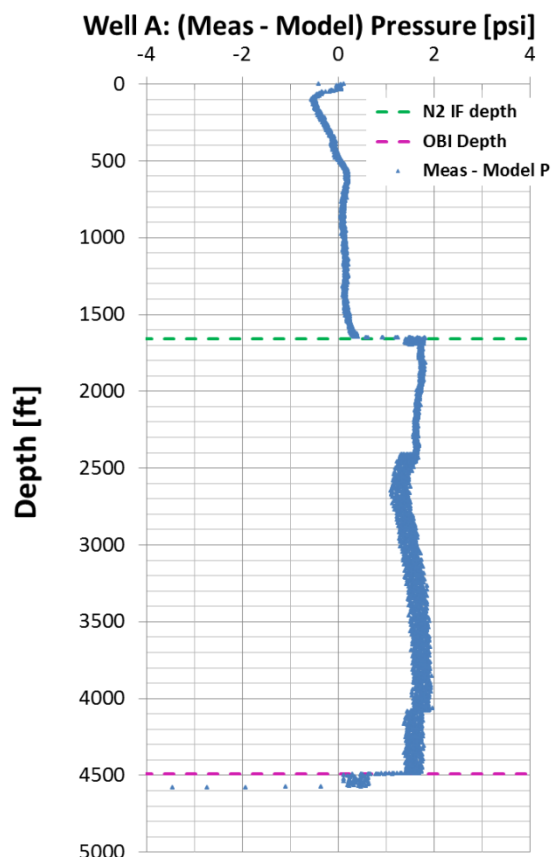


Figure 6-2: Graphic of the difference between measured pressure data from the log (as a function of depth) at initialization of the test vs. the predicted pressure from the model.

Once the model was calibrated, a change in cavern pressure (brine pressure) was simulated with the assumption of no fluid mass loss. The model predictions for nitrogen wellhead pressures and NOI as a function of the changes in cavern pressure are shown in Table 6-2. During the 28 days test the cavern pressure variation (taken as the change in pressure at the brine string wellhead) was +8 psi. The relative pressurization rates for the nitrogen filled wells are given in Table 6-3.

The model was able to capture the magnitude of the wellhead pressure reasonably well (see Figure 6-3), but closer analysis of the pressurization rates shows slight difference in their rates. In fact, it was found that the pressurization rate for well A is slightly higher than the range found from the analysis of the measured data. The fact that the model can still predict the magnitude of the pressure in well A reasonably well is due to the relatively short duration of the test. The model and DCS pressure values match at initialization and the small difference in pressure slopes is not enough to show a large drift from the measured data after only 8 psi (or the 28 days duration of the test). The pressure prediction for well B, on the other hand, seems to fall in within the experimental data range. An offset in the predicted NOI for well A was also found. A number of possible reasons for the discrepancy are given in section 6.3.

Table 6-2: Model predictions for the wellhead pressure and NOI for both wells. The value of pressure at initialization was set to match.

Parameter	Well A		Well B	
	Initialization	Finalization	Initialization	Finalization
NOI Model [ft]	1657.0	1650.7	2418.1	2418.0
NOI Experiment [ft]	1649	1636	2419	2419
Pressure (model) [psi]	1583	1588.8	1809	1816.4
Pressure (experiment) [psi]	1583	1587	1809	1816

Table 6-3: Relative pressurization rates for WH117A and WH117B predicted by the hydrostatic column model as they compare to the experimental data.

Parameter	WH117A N2	WH117B N2	WH117B Brine
P(oil)/P(B, brine) (model)	0.732	0.924	1
P(oil)/P(B, brine) (experiment)	0.58-0.68	0.90-1.0	1

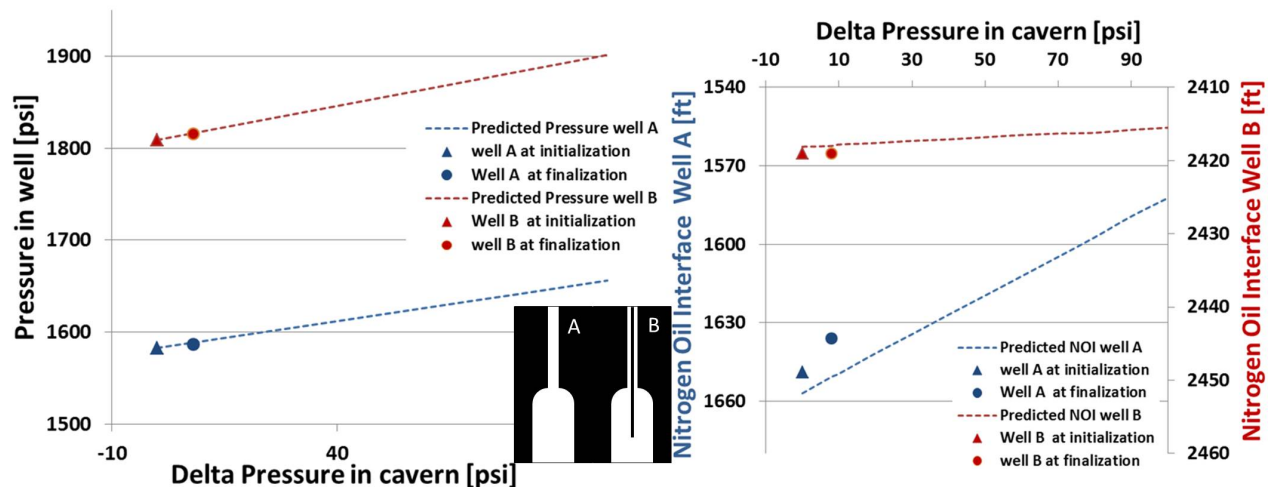


Figure 6-3: Wellhead pressure (left) and NOI (right) for WH117A and B as predicted from the nitrogen column model and compared to the measured values.

6.3 Possible Source of Discrepancy

There are a number of possible explanations for discrepancy between the model predictions and the measured during the test. Some are related to approximations that were used in the model development, while others are related to the system and uncertainties in the logging measurements. Following is a list the possibilities we have considered. A detailed discussion on each one is beyond the scope of this report and will be included in a subsequent report detailing the design and function of the hydrostatic column model and applications to SPR. Many of these were downgraded in likelihood or impact upon calibrating the model to the measured wireline data.

1. Model Inaccuracies
 - a. Math error in the programming (programming bug)
 - b. Linear correction to $\rho = f(T,P)$ not accurate enough. Non-linearity not captured.
 - c. E not constant, rather $E = f(T,P)$
 - d. β not constant
 - e. Ideal gas law inaccuracies. Not good enough in this application, $Z \neq 1.04$
 - f. R value for N_2 may be off
 - i. Pure N_2 assumption incorrect
 - ii. Hydrocarbon gasses diffused into N_2
 - g. Zone sizes in the model are too coarse to capture smaller details
 - h. Hydrostatic assumption breaks down in some zones, especially in region of strongest temperature gradient
2. Measurement inaccuracies
 - a. Pressure at the wellhead (DCS)
 - b. P , T , γ from wireline
 - c. Wellbore geometry (ID @depth)
 - d. Wireline stretch
 - e. Interface measurements (possible shifts)
3. Data analysis (fitting to pressure data)
4. N_2 -oil interactions (mass diffusion)
5. Small Mass (N_2) leak

6.4 Model Estimates for Possible N₂ Leak Rates

The hydrostatic column model was used to explore how wellhead pressurization rates and interface displacement rates should compare with brine pressurization rates given known well geometry and assumed leak rates. This gives the authors a measure of what magnitude of leak rate (mass or volume of gas per unit time) should correspond with what relative pressurization rate.

6.4.1 Well A simulations

The hydrostatic column model was used to predict the wellhead pressurization rates and NOI displacement rates for a number of small hypothetical N₂ leak rates below current MIT detection limits. One of the possible explanations for the relative pressurization rates observed on Well A falling below the theoretical 0.73 (recall Table 6-3) is the existence of a small N₂ leak in well A somewhere above the casing shoe. For the model runs, the leak rate (Δ N₂ mass/time) was assumed to be constant with time and the largest simulated leak rate was equivalent to the MDLR, which for the case of WH117A was 448 kg/yr (or 23.5 bbl/yr at casing seat depth P,T conditions). A summary of the model-calculated pressurization rates (columns 3,4) and NOI displacement rates (column 5) as functions of leak rates (columns 1,2) are shown in Table 6-4. Also, for reference, a table with nitrogen density at well conditions and conversion factors for leaks rates is included in the Appendix: Conversions. The calculated relative pressurization rate appears to be quite sensitive to leak rates examined in this way.

Table 6-4: Summary of predicted pressurization rates as a function of calculated leak rates. N₂ leak rate volumes [bbl/yr] in column 1 are given at casing seat depth P, T conditions.

Leak rate		Pressurization rate	Relative Pressurization rate	Interface displacement rate
[bbl/yr]	[kg/yr]	[psi/day]	[psi/psi]	[ft]/28 days
0	0	0.21	0.73	6.3
2.5	47.6	0.20	0.69	7.0
10	191.6	0.17	0.58	9.9
20.5	391.1	0.12	0.43	14.0
23.5	448.4	0.11	0.39	15.3

The data from Table 6-4 are plotted in Figure 6-4 for graphical presentation. The horizontal axis in this new plot represents cavern pressure. The 1:1 pressurization rate is shown with a solid black line. The theoretical tight cavern relative pressurization rate, $P(A_{oil})/P(B, \text{brine}) = 0.73$ is shown with the solid blue line that forms the upper bound of the shaded area. This theoretical value is a function of the geometry of the well, its pressure, and the location of the NOI, and it can vary from well to well. The lower bound of the shaded area was set to the MDLR and represents the minimum relative pressurization rate that can be detected by an MIT. Again, this is going to be a specific value for each well, and in this case was taken to be 23.5 bbl/yr according to the 2014 MIT report on WH117(McCoy 2014). A gas leak rate above 0 bbl/yr but

below the MDLR should create a relative pressurization curve that falls into the shaded area. Recall the leak point must sit above the NOI for this model to apply.

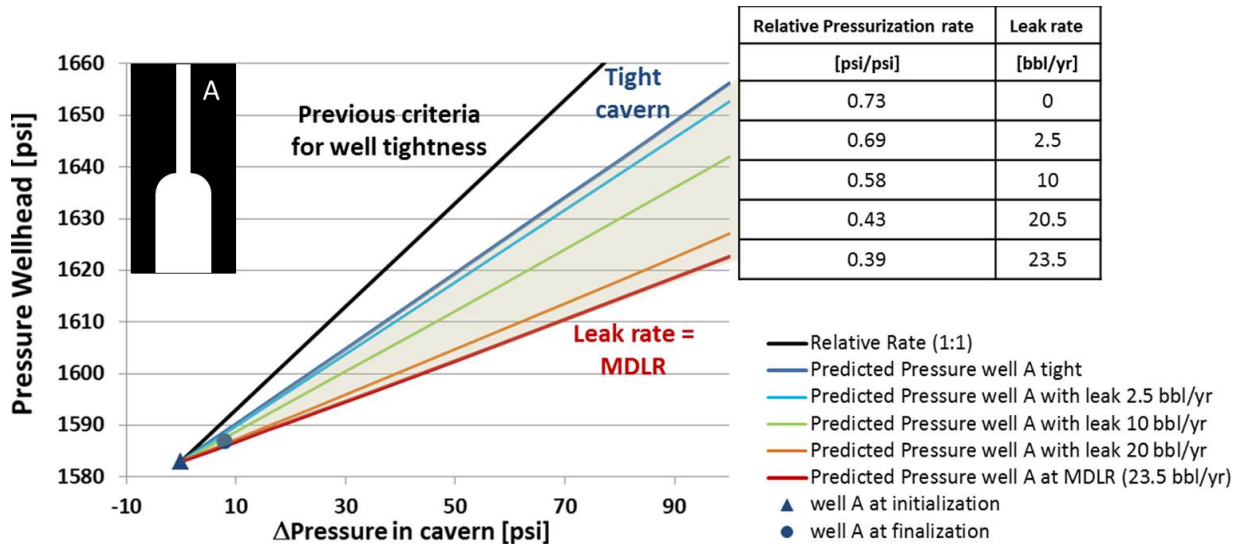


Figure 6-4: Wellhead pressure prediction for WH117A as a function of the change in cavern pressure. Listed on the table on the right are the relative pressurization rates and the corresponded apparent leak rates.

To visually compare the DCS pressure data to the model prediction we converted the change in pressure into times by using an apparent linearized cavern pressurization rate. From the test we know that the brine pressure increased by 8 psi in 28 days yielding a rate of 0.286 psi/day. This factor is used to produce Figure 6-5. The DCS pressure measurements are found to be within the range of pressures still considered tight from the MIT, but on average correspond to a leak rate ~ 20 bbl/yr.

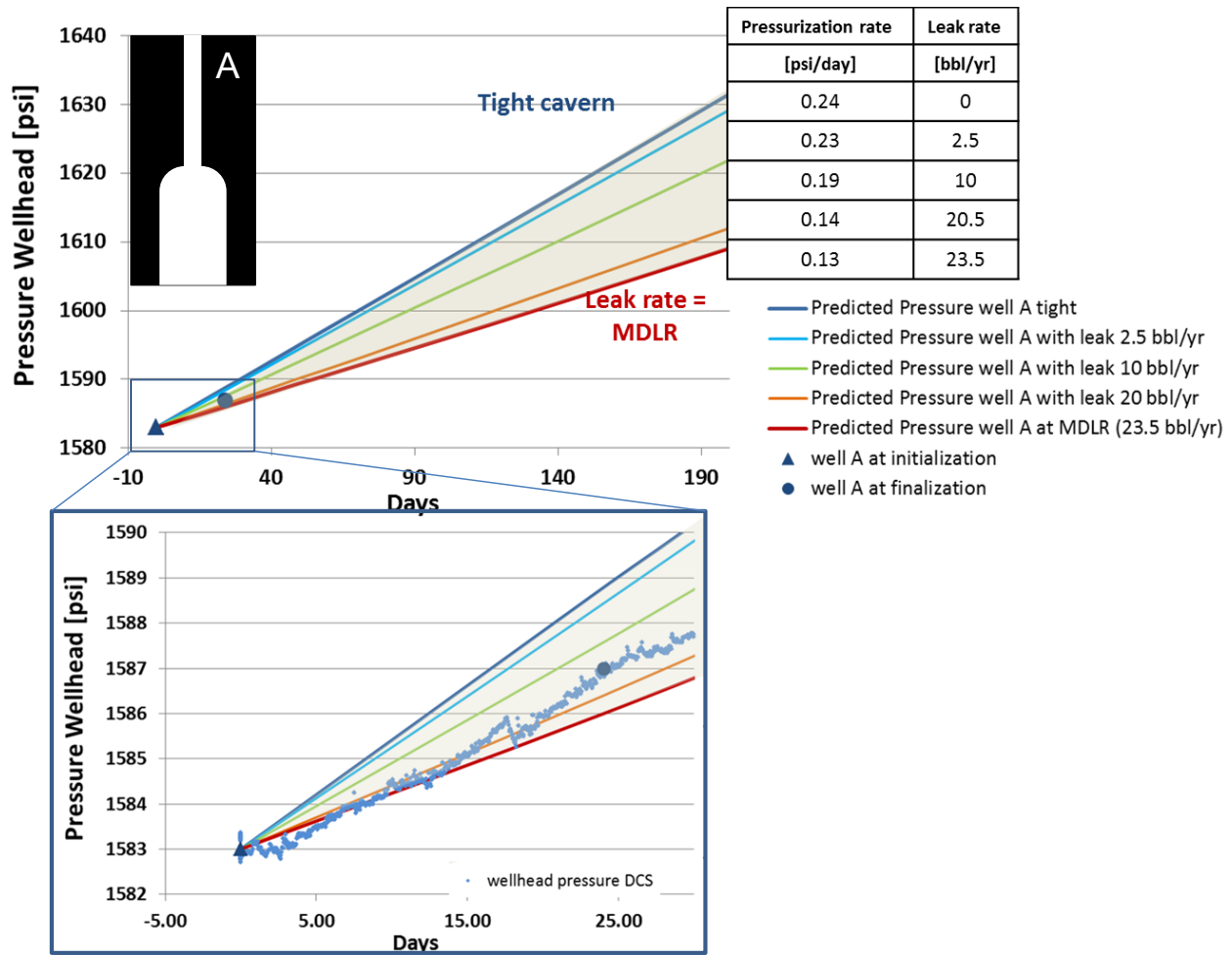


Figure 6-5: Pressure prediction as a function of time for WH117A. Inset view shows model predictions during the nitrogen test as it compared to the observed wellhead pressure data.

As previously discussed, the model also predicts the position of the NOI as a function of time and assumed leak rates, illustrated graphically in Figure 6-6. It is apparent from this plot that the model is not capable to exactly predict the NOI at the initialization point, and an offset between measured and predicted of about 8 ft. was found. The reason for this offset is still under investigation and an in-depth analysis of all model parameters is planned. None the less, we can still look at the relative movement of the NOI during the test and relate it to the predicted interface movement by the model. We find that the model-predicted NOI displacement at test finalization ranges from 6.3 ft for a tight well to 15.3 ft. for a well leaking at the MDLR (23.5 bbl/yr N_2). The measured 13 ft. NOI displacement has an associated measurement uncertainty reported to be ± 0.5 ft., which propagates into a range consistent with calculated leak rates that vary from 17.3 to 22.5 bbl/yr (see right table in Figure 6-6). This brackets the ~ 20 bbl/yr leak rate estimated from the model predictions developed from matching the average slope of the pressure history. The model therefore suggests that that the interface movement and pressurization history in the A-well could both be explained by a ~ 20 bbl/yr N_2 leak rate.

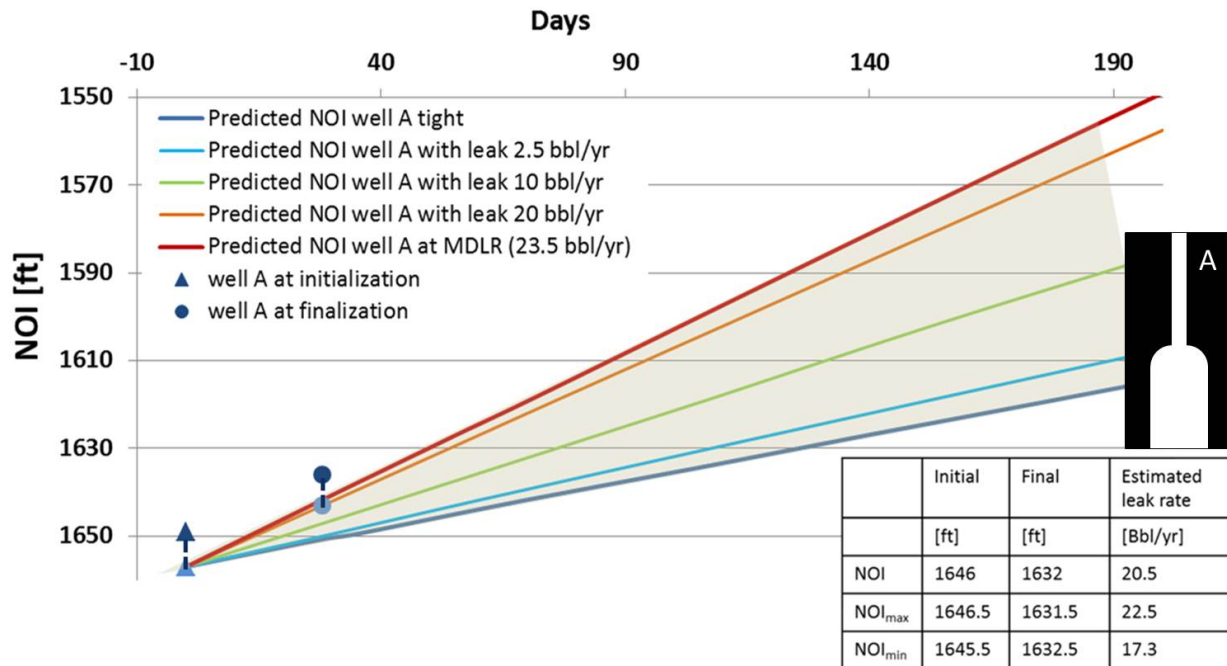


Figure 6-6: Prediction of the NOI movement for a range of simulated leak rates. Table illustrates how an uncertainty of ± 0.5 ft in the NOI measurement can lead to an estimated leak rates that varies between 17.3-22.5 bbl/yr.

6.4.2 Well B

The hydrostatic column model was also used to run a small leak analysis for the B well. The major differences between the A- and B- wells are that the NOI for well B is below the casing shoe and a few feet inside the chimney of the cavern. Also, it contains the brine string and therefore the effective cross sectional area in the cased well section is much smaller than in well A.

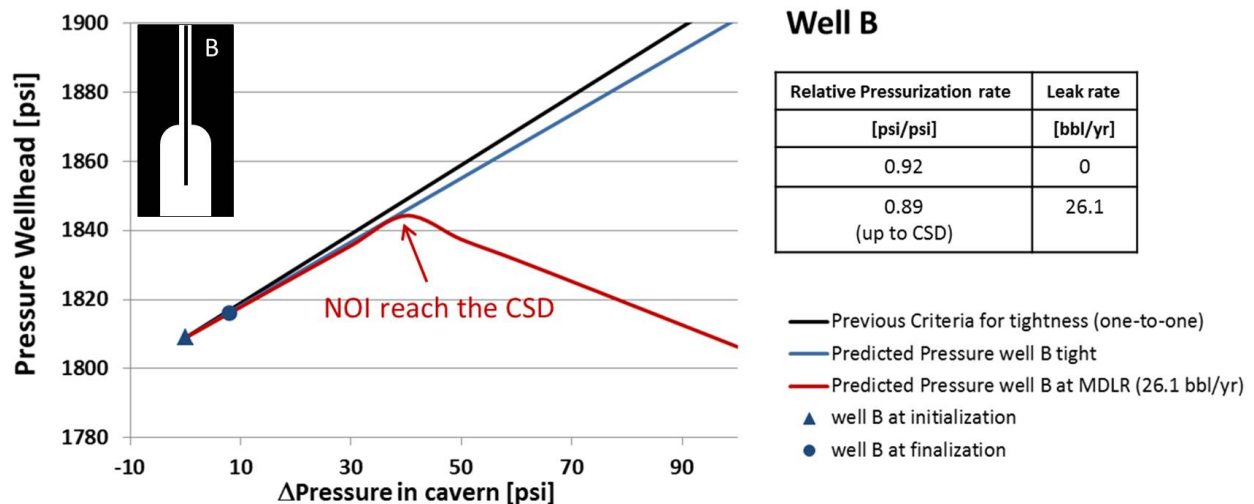


Figure 6-7: Wellhead pressure prediction for WH117B. (right) table with the simulated leak rate and resultant relative pressurization rate.

The prediction for the ‘tight’ wellhead pressurization rate of 0.92 (shown in blue in Figure 6-7) is much different than in the rate of 0.73 in well A in that it is much closer to a slope = 1.0. As mentioned earlier, this is due to the different conditions in the well and location of the NOI. A detailed study on the parameters that affect this theoretical tight pressurization rate is planned for the near future and will be included in a final Hydrostatic Column Model report.

A leak of the value of the MDLR was simulated with the model, and predicted wellhead pressure is shown in red in Figure 6-7. The relative pressurization rate at this leak is calculated to be 0.89 until the NOI reaches the casing shoe depth and the effective area at depth shrinks dramatically. This creates a very fast moving NOI and a resultant pressure drop; the predicted movement of the NOI is shown in Figure 6-8. The measurements for the NOI at initialization (2419±1 ft) and finalization (2419±1 ft) support the model prediction of a tight well.

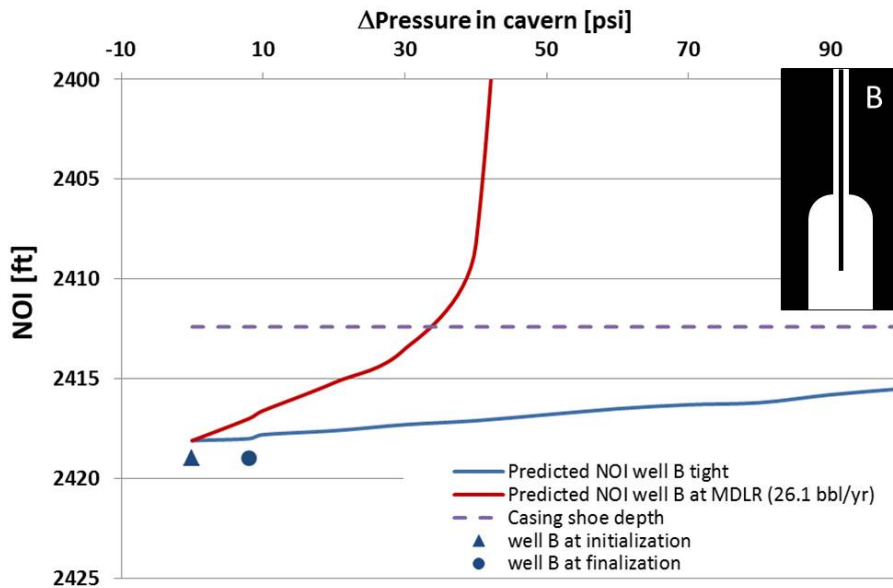


Figure 6-8: WH117B NOI predictions for a tight well (blue) and a simulated leak (red) of 26.1 bbl/yr. Dashed line corresponds to the Casing Shoe Depth.

7 Conclusion

A number of conclusions can be drawn by comparing the measured data from the wireline logs and DCS to the model predictions. The major points are summarized as followed:

1. Wells under long term nitrogen monitoring with the NOI up in the relatively narrow cased hole do not pressurize with a relative rate ($P(N_2)/P(\text{brine})$) of 1.
 - a. This analysis confirms that the differences in compressibility between nitrogen and the cavern filled fluid drives the nitrogen pressure to rise at a lower rate.
 - b. The Theoretical Tight Pressurization Rate (TTPR) depends on the well configuration, pressure and location of the NOI and varies from well to well.
 - c. For the specific case of WH117 during the post-MIT period:
 - i. $TTPR_A = 0.73$
 - ii. $TTPR_B = 0.92$
2. High resolution wireline data helped validate the hydrostatic column model that was used to predict the nitrogen pressure along the entire fluid column from BHF to bottom of brine pool.
3. According to the model prediction:
 - a. Well A pressurization rate and NOI displacement observed during the special test period are consistent with a loss rate of ~ 20 bbl/yr of nitrogen, which is smaller than the detection limit of MDLR = 23.5 bbl/yr from the January 2014 MIT
 - b. Well B pressurization and interface movement is consistent with no loss of nitrogen over the test period.
4. The model combined with long term nitrogen monitoring can be used as a very sensitive tool to differentiate apparent leaks smaller than the reported MDLR.
5. The same approach may be applied to the suite of caverns currently under nitrogen monitoring at Big Hill to help differentiate which wells still remain suspect versus those that appear to be tight
6. Direct validation of nitrogen leak rates between 0 and MDLR should be performed in the future on SPR well in order to demonstrate the accuracy of the model in calculating leaks

As a closing comment, the authors feel it important to note that pressure testing is only one part of a responsible well integrity monitoring program. Wells that are tight under nitrogen do not have an associated forecast for future performance. Other parameters such as the casing deformation, age and performance as compared to similar wells, cemented annulus pressures, and geomechanical model evaluations all play a role in risk management and mitigation.

8 Cited References

- Ballard, S. and B. Ehgartner (2000). "Caveman Version 3.0; A Software System for SPR Cavern Pressure Analysis." *Unlimited Release SAND2000-1751*. Sandia National Laboratories, Albuquerque, NM.
- Berest, P., B. Brouard and G. Durup (2002). "Tightness Tests in Salt-Cavern Wells." *presented at SMRI Spring 2002 Technical Conference*, Banff, Alberta, Canada, 28-April-2002, Solution Mining Research Institute.
- Cassidy, A. (2010). "Casing Inspection Analysis WH117A." Weatherford, New Orleans, LA USA. U.S. Strategic Petroleum Reserve.
- Ehgartner, B. L. (2004). "Incorporation of Compressibility Model and other Enhancements/Upgrades into Caveman." Geotechnology & Engineering Department, Sandia National Laboratories, Albuquerque, NM. U.S. Strategic Petroleum Reserve. March 31, 2004.
- Ehgartner, B. L. (2003). "Review of CAVEMAN - Recommended Upgrades." Geotechnology & Engineering Department. Sandia National Laboratories, Albuquerque, NM 87185-0706. U.S. Strategic Petroleum Reserve. 24-Oct-2003.
- Franks, D. G. (1984a). "Well History Well No.117A." **WH6443.117001**. Jacobs/D'appolonia Engineers, New Orleans, LA USA. U.S. Strategic Petroleum Reserve.
- Franks, D. G. (1984b). "Well History Well No.117B " **WH6443.117002**. Jacobs/D'appolonia Engineers, New Orleans, LA USA. U.S. Strategic Petroleum Reserve.
- McCoy, M. (2014). "Cavern Integrity Test Report West Hackberry 117." **AAA9020.536**, Cavern Integrity Group. DM Petroleum Operations, New Orleans, LA. U.S. Strategic Petroleum Reserve. 2-Feb-2014.
- Sonntag, R. E. and G. J. Van Wylen (1991). Introduction to thermodynamics : classical and statistical. New York, J. Wiley.

Figure 9-1 West Hackberry 117A, Well Completion Configuration Drawing, WH-M-123-041, 5/5/2014





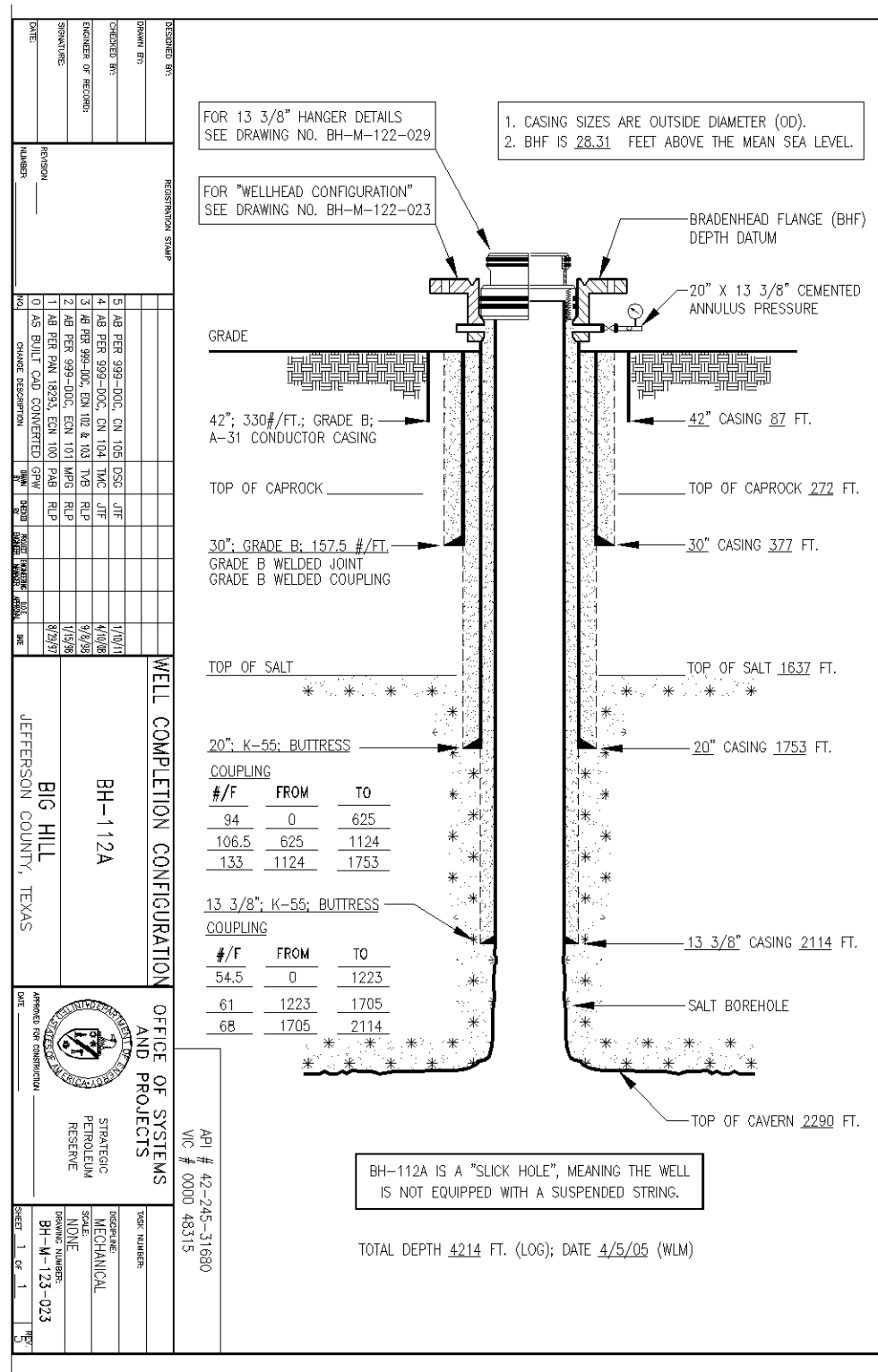


Figure 9-3. Big Hill-112A, Well Completion Configuration, Drawing BH-M-123-023, version 5, 1/10/2011.



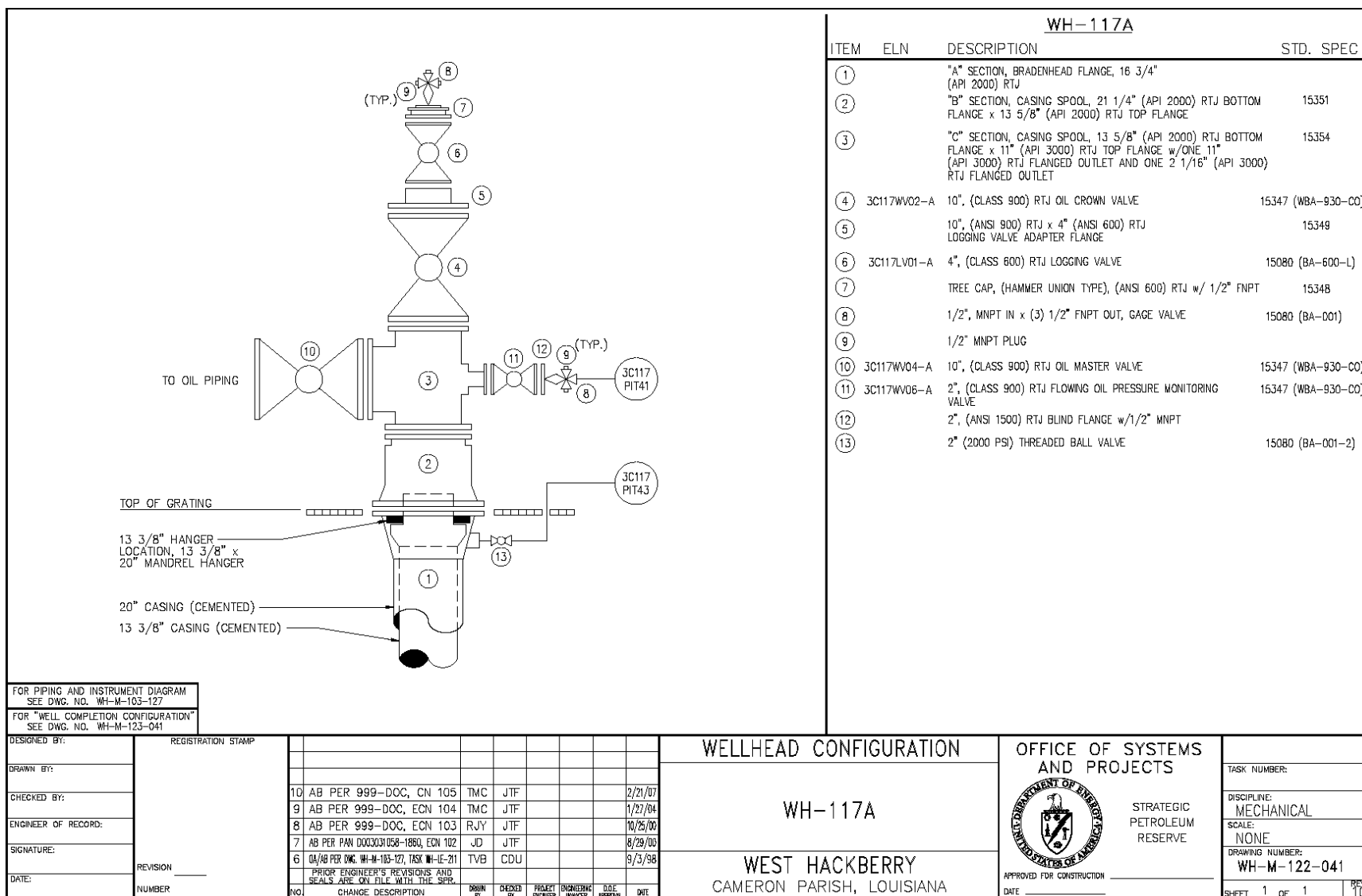


Figure 9-5. West Hackberry 117A, Wellhead Configuration Drawing, WH-M-122-041, 2/21/2007

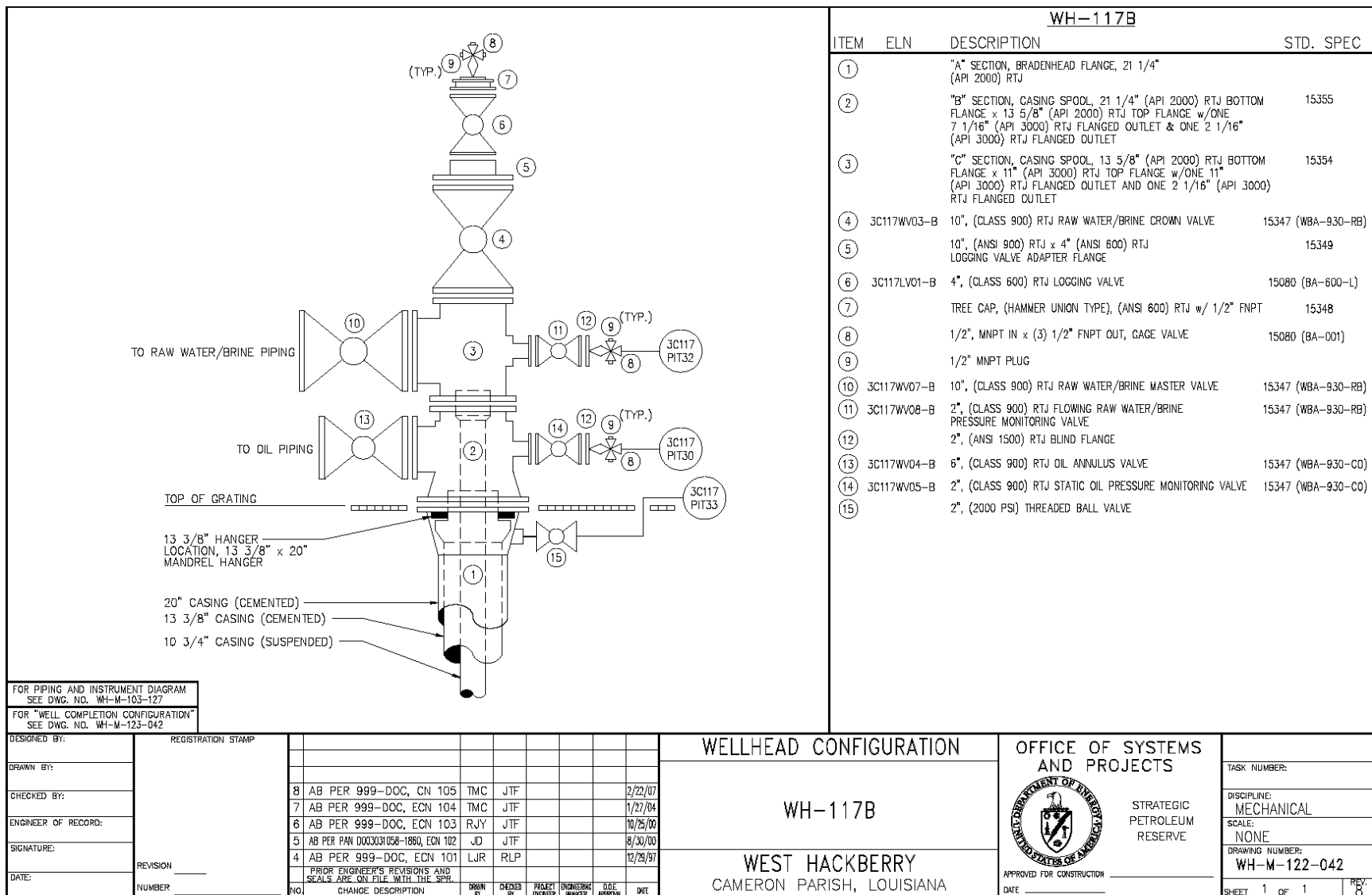


Figure 9-6. West Hackberry 117B, Wellhead Configuration Drawing, WH-M-122-042, 2/22/2007

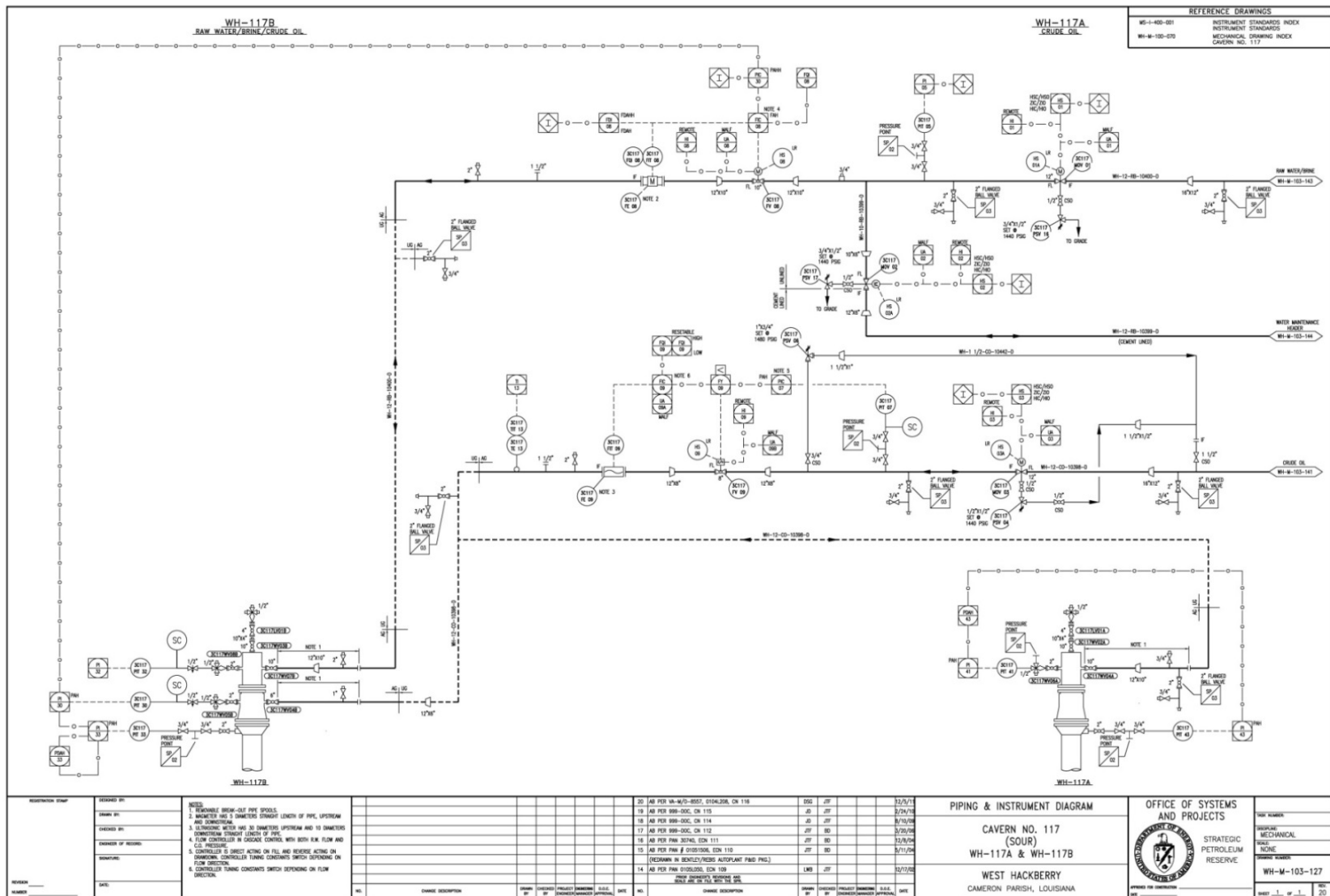


Figure 9-7. WH117, Piping and Instrument Drawing, WH-M-103-127, 12/5/2011

10 Appendix: Logs

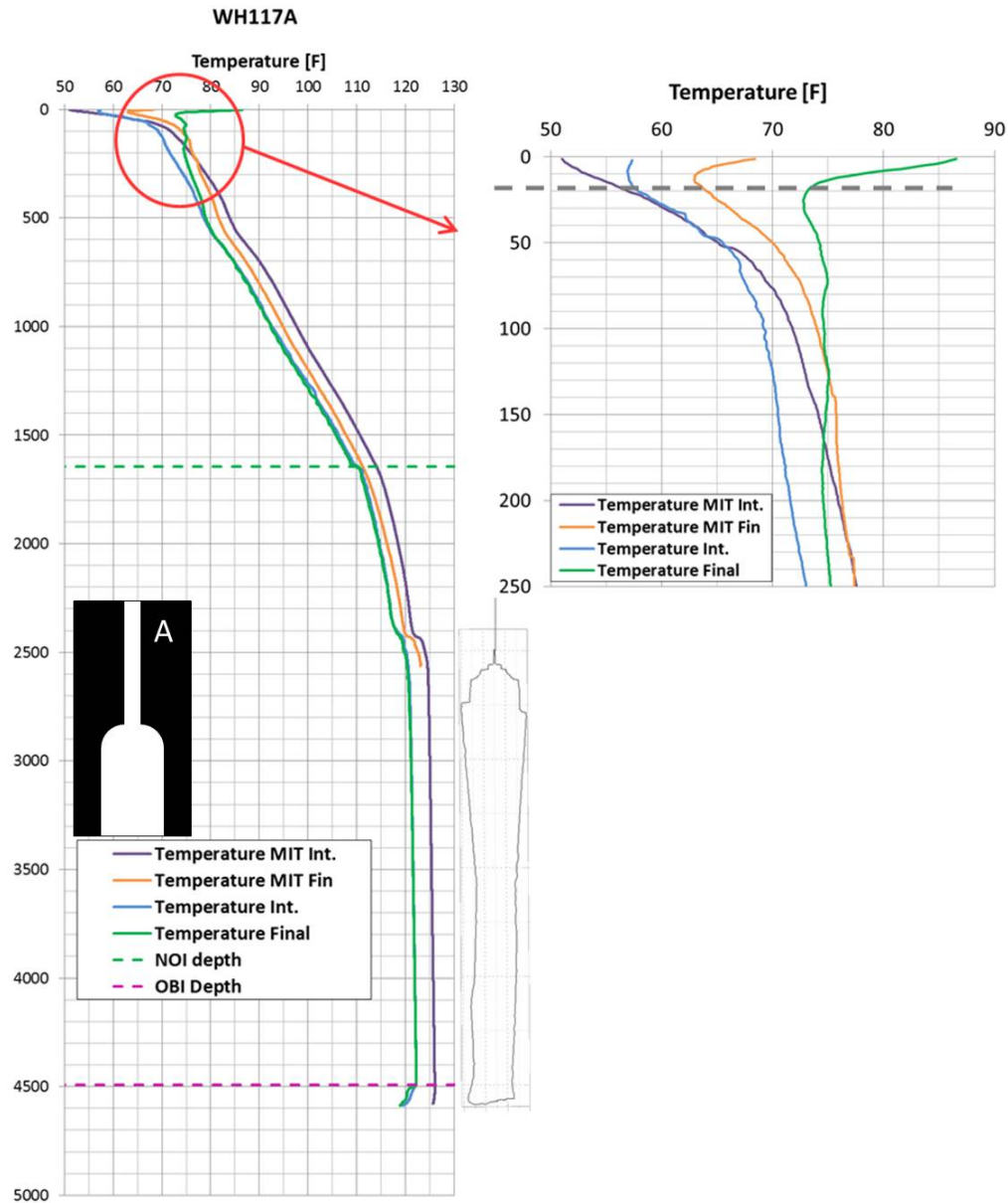


Figure 10-1. Temperature logs for WH117A since December 2013.

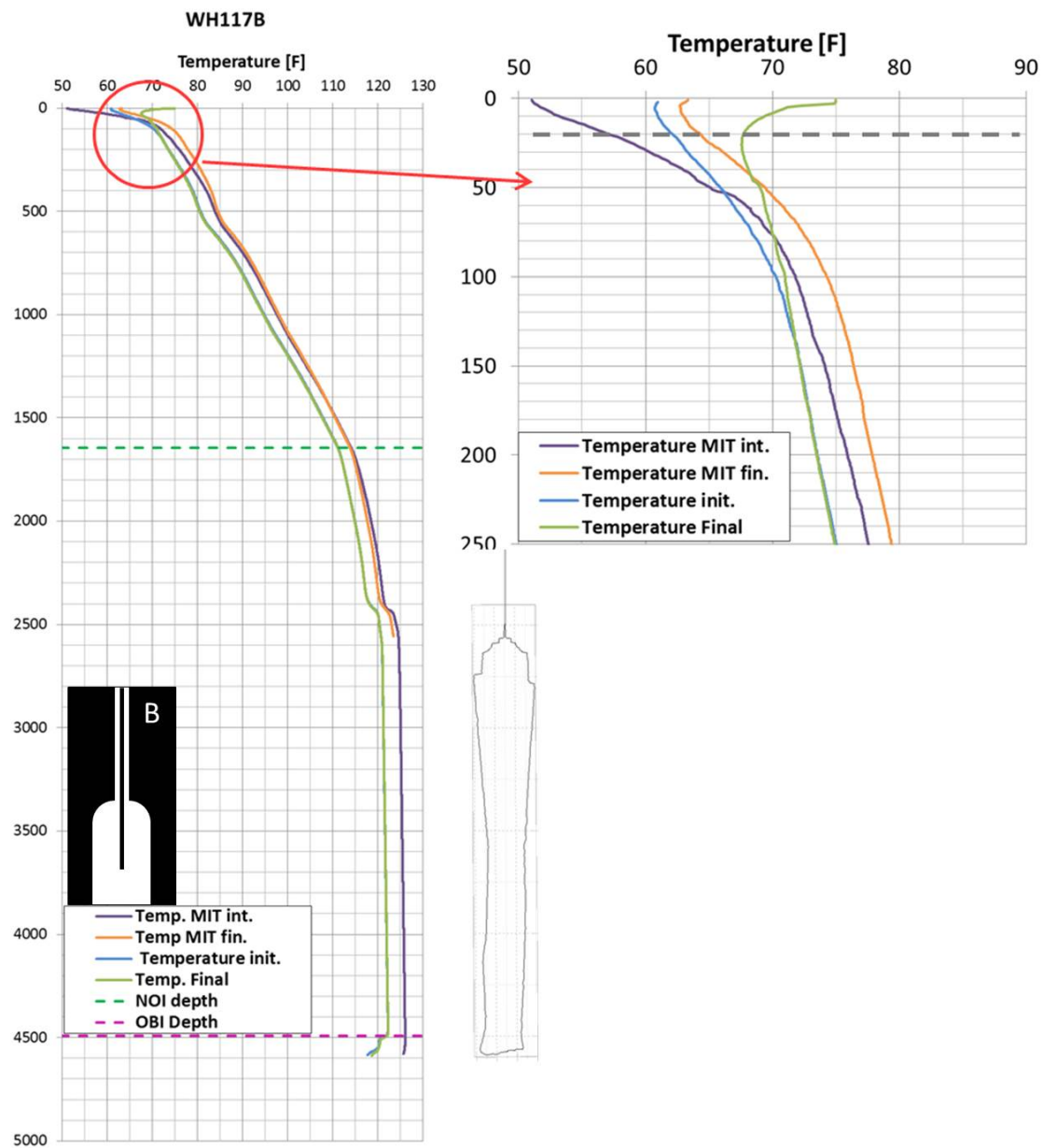


Figure 10-2. Temperature logs for WH117B since December 2013.

11 Appendix: Oil Quality

Table 11-1. Crude oil inspection analysis for WH117 (July, 2002)

SPR CRUDE OIL INSPECTION ANALYSIS											
Date Started	7/30/2002		Sample ID	West Hackberry, Cavern 117			-	-	Date Reported		8/8/2002
			Sp. Gr.		Pour Pt.	Nitrogen	Sulfur	Sulfur	Viscosity		Water
Sample No.			D 5002	Gravity	D 5853	D 5762	D 1552/IR	D 4294/XRF	centistokes, D 445		D 4928
Date Collected	Bottle Label	Depth (ft.)	at 60/60° F	°API	°F	(wt. %)	(wt. %)	(wt. %)	at 77° F	at 100° F	(wt. %)
2002SPR084 7/17/02	WH02717-004	2560	0.8551	34.0	-5	0.128	1.17	1.339	7.800	5.351	0.02
2002SPR085 7/17/02	WH02717-003	2800	0.8567	33.7	0	0.129	1.27	1.338	8.113	5.531	0.11
2002SPR086 7/17/02	WH02717-002	3040	0.8564	33.7	-10	0.125	1.22	1.308	8.023	5.463	0.04
2002SPR087 7/17/02	WH02717-001	3281	0.8564	33.7	-5	0.132	1.26	1.316	8.071	5.475	0.25
2002SPR088 7/16/02	WH02716-005	3521	0.8552	34.0	5	0.131	1.25	1.312	7.767	5.375	0.05
2002SPR089 7/16/02	WH02716-004	3761	0.8556	33.9	5	0.138	1.26	1.300	7.809	5.361	0.05
2002SPR090 7/16/02	WH02716-003	4001	0.8563	33.7	0	0.130	1.19	1.342	8.032	5.463	0.08
2002SPR091 7/16/02	WH02716-002	4051	--	--	--	--	Sludge	--	--	--	5.37
2002SPR092 7/16/02	WH02716-001	4055	--	--	--	--	Sludge	--	--	--	11.05
2002SPR093 7/15/02	WH02715-003	4056	--	--	--	--	Sludge	--	--	--	10.58
2002SPR094 7/15/02	WH02715-002	4057	1.2065	--	--	--	Brine	--	--	--	--
2002SPR095 7/15/02	WH02715-001	4061	1.2067	--	--	--	Brine	--	--	--	--
				33.812			1.231				

12 Appendix: Model Well Geometry

Table 12-1. West Hackberry 117A well geometry

Interval	Upper [ft]	Lower [ft]	Annular Space		Area [ft ²]	Seg Vol [ft ³]	Cum Vol [ft ³]	Area[m ²]	Upper [m]	Lower [m]	dZ [m]	OD [m]	ID [m]	Comment
1	0	500	1.04	0	0.85	427	427	0.079	0.0	152.4	0.5000	0.32	0	cased hole
2	500	1500	1.04	0	0.85	1281	1709	0.079	152.4	457.2	0.3048	0.32	0	cased hole
3	1500	1600	1.04	0	0.85	1367	3075	0.079	457.2	487.7	0.3048	0.32	0	cased hole
4	1600	1700	1.04	0	0.85	1452	4528	0.079	487.7	518.2	0.1250	0.32	0	cased hole
5	1700	1800	1.04	0	0.85	1538	6065	0.079	518.2	548.6	0.3048	0.32	0	cased hole
6	1800	1900	1.04	0	0.85	1623	7688	0.079	548.6	579.1	0.3048	0.32	0	cased hole
7	1900	2000	1.04	0	0.85	1709	9397	0.079	579.1	609.6	0.3048	0.32	0	cased hole
8	2000	2100	1.04	0	0.85	1794	11191	0.079	609.6	640.1	0.3048	0.32	0	cased hole
9	2100	2200	1.04	0	0.85	1879	13070	0.079	640.1	670.6	0.3048	0.32	0	cased hole
10	2200	2220	1.04	0	0.85	1896	14967	0.079	670.6	676.7	0.3048	0.32	0	cased hole
11	2220	2240	1.04	0	0.85	1914	16880	0.079	676.7	682.8	0.3048	0.32	0	cased hole
12	2240	2260	1.04	0	0.85	1931	18811	0.079	682.8	688.8	0.3048	0.32	0	cased hole
13	2260	2300	1.04	0	0.85	1965	20776	0.079	688.8	701.0	0.3048	0.32	0	cased hole
14	2300	2350	1.04	0	0.85	2008	22783	0.079	701.0	716.3	0.3048	0.32	0	cased hole
15	2350	2360	1.04	0	0.85	2016	24799	0.079	716.3	719.3	0.3048	0.32	0	cased hole
16	2360	2380	1.04	0	0.85	2033	26832	0.079	719.3	725.4	0.3048	0.32	0	cased hole
17	2380	2400	1.04	0	0.85	2050	28882	0.079	725.4	731.5	0.3048	0.32	0	cased hole
18	2400	2410	1.04	0	0.85	2059	30941	0.079	731.5	734.6	0.3048	0.32	0	cased hole
19	2410	2415	1.04	0	0.85	2063	33004	0.079	734.6	736.1	0.3048	0.32	0	cased hole
20	2415	2416	2.37	0	4.40	10630	43635	0.409	736.1	736.4	0.0500	0.72	0	upper chimney
21	2416	2417	2.88	0	6.50	15711	59345	0.604	736.4	736.7	0.0500	0.88	0	upper chimney
22	2417	2418	3.11	0	7.60	18377	77722	0.706	736.7	737.0	0.0500	0.95	0	upper chimney
23	2418	2419	3.29	0	8.50	20562	98283	0.790	737.0	737.3	0.0500	1.00	0	upper chimney
24	2419	2420	3.40	0	9.10	22022	120305	0.845	737.3	737.6	0.0500	1.04	0	upper chimney
25	2420	2421	3.51	0	9.70	23484	143789	0.901	737.6	737.9	0.0500	1.07	0	upper chimney
26	2421	2422	3.57	0	10.00	24220	168009	0.929	737.9	738.2	0.0500	1.09	0	upper chimney
27	2422	2473	3.62	0	10.30	25472	193481	0.957	738.2	753.8	0.1250	1.10	0	upper chimney
28	2473	2563	3.76	0	11.10	28449	221930	1.031	753.8	781.2	0.5000	1.15	0	middle chimney
29	2563	4489	200.00	0	31415.93	141026094	141248025	2918.635	781.2	1368.2	0.5000	60.96	0	Cavern
30	4489	4500	200.00	0	31415.93	141371669	282619694	2918.635	1368.2	1371.6	0.1000	60.96	0	near OBI
31	4500	4550	200.00	0	31415.93	142942466	425562160	2918.635	1371.6	1386.8	0.5000	60.96	0	Cavern
32	4550	4595	200.00	0	31415.93	144356182	569918342	2918.635	1386.8	1400.6	0.5000	60.96	0	Cavern

Table 12-2. West Hackberry 117B well geometry

Interval	Upper [ft]	Lower [ft]	Annular Space OD [ft]	ID [ft]	Area [ft ²]	Seg Vol [ft ³]	Cum Vol [ft ³]	Area[m ²]	Upper [m]	Lower [m]	dZ [m]	OD [m]	ID [m]	Comment
1	0	500	1.04	0.90	0.22	112	112	0.021	0	152.4	0.5	0.32	0.27	cased hole
2	500	1500	1.04	0.90	0.22	336	448	0.021	152.4	457.2	0.3048	0.32	0.27	cased hole
3	1500	1600	1.04	0.90	0.22	358	806	0.021	457.2	487.68	0.3048	0.32	0.27	cased hole
4	1600	1700	1.04	0.90	0.22	381	1187	0.021	487.68	518.16	0.3048	0.32	0.27	cased hole
5	1700	1800	1.04	0.90	0.22	403	1590	0.021	518.16	548.64	0.3048	0.32	0.27	cased hole
6	1800	1900	1.04	0.90	0.22	426	2016	0.021	548.64	579.12	0.3048	0.32	0.27	cased hole
7	1900	2000	1.04	0.90	0.22	448	2464	0.021	579.12	609.6	0.3048	0.32	0.27	cased hole
8	2000	2100	1.04	0.90	0.22	470	2934	0.021	609.6	640.08	0.3048	0.32	0.27	cased hole
9	2100	2200	1.04	0.90	0.22	493	3427	0.021	640.08	670.56	0.3048	0.32	0.27	cased hole
10	2200	2220	1.04	0.90	0.22	497	3924	0.021	670.56	676.656	0.3048	0.32	0.27	cased hole
11	2220	2240	1.04	0.90	0.22	502	4425	0.021	676.656	682.752	0.3048	0.32	0.27	cased hole
12	2240	2260	1.04	0.90	0.22	506	4932	0.021	682.752	688.848	0.3048	0.32	0.27	cased hole
13	2260	2300	1.04	0.90	0.22	515	5447	0.021	688.848	701.04	0.3048	0.32	0.27	cased hole
14	2300	2350	1.04	0.90	0.22	526	5973	0.021	701.04	716.28	0.3048	0.32	0.27	cased hole
15	2350	2360	1.04	0.90	0.22	529	6502	0.021	716.28	719.328	0.3048	0.32	0.27	cased hole
16	2360	2380	1.04	0.90	0.22	533	7035	0.021	719.328	725.424	0.3048	0.32	0.27	cased hole
17	2380	2400	1.04	0.90	0.22	538	7572	0.021	725.424	731.52	0.3048	0.32	0.27	cased hole
18	2400	2410	1.04	0.90	0.22	540	8112	0.021	731.52	734.568	0.3048	0.32	0.27	cased hole
19	2410	2412	1.04	0.90	0.22	540	8652	0.021	734.568	735.1776	0.125	0.32	0.27	cased hole
20	2412	2416	3.83	0.90	10.91	26360	35012	1.014	735.1776	736.3968	0.05	1.17	0.27	upper chimney
21	2416	2419	3.92	0.90	11.42	27620	62632	1.061	736.3968	737.3112	0.05	1.19	0.27	upper chimney
22	2419	2560	4.00	0.90	11.94	30556	93189	1.109	737.3112	780.288	0.125	1.22	0.27	lower chimney
23	2560	4596	200.00	0.90	31415.30	144384702	144477890	2918.577	780.288	1400.861	0.5	60.96	0.27	cavern

13 Appendix: Conversions

Wellhead pressure [psig]	Pressure at CSD (2415 ft) [psig]	ρ_{N_2} at surface [kg/m ³]	ρ_{N_2} at CSD [kg/m ³]	Leak mass/volume [kg/bbl]
Atmospheric Pressure		1.15		0.18
1400	1511	110.0	106.0	17.27
1500	1619	117.9	113.5	18.51
1600	1727	125.7	121.0	19.73
1700	1835	133.4	128.5	20.94
1800	1943	141.2	136.2	22.17
1900	2051	149.0	143.5	23.40

Pressure and density values were acquired by using column model with temperature log taken on March 27th, 2014. According to the log the temperature at casing shoe depth (CSD) was 119.2 F, while it was 57 F at the Braden Head Flange (BHF).

Distribution

External Distribution

Electronic copies to:

Wayne Elias (wayne.elias@hq.doe.gov) for distribution to DOE SPR Program Office, Washington, DC

Diane Willard (diane.willard@spr.doe.gov) for distribution to DOE and FFPO SPR Project Management Office, New Orleans, LA

Sandia Distribution

Electronic copies to:

MS0899 Technical Library. 9536

